Macrophage and dendritic cell subset composition can distinguish endotypes in adjuvant-induced asthma mouse models

Müge Özkan[1], Yusuf Cem Eskiocak[2], Gerhard Wingender[2,3*]

[1] Department of Genome Sciences and Molecular Biotechnology, Izmir International Biomedicine and Genome Institute, Dokuz Eylul University, 35340 Balcova/Izmir, Turkey;

[2] Izmir Biomedicine and Genome Center (IBG), 35340 Balcova/Izmir, Turkey.

[3] Department of Biomedicine and Health Technologies, Izmir International Biomedicine and Genome Institute, Dokuz Eylul University, 35340 Balcova/Izmir, Turkey.

* Correspondence: gerhard.wingender@ibg.edu.tr (G.W.)

Keywords:

Asthma, endotypes, pDC, interstitial macrophages, exudate macrophages

Abbreviations:

AM: alveolar macrophage; BALF: bronchoalveolar lavage fluid; CFA: complete Freud's adjuvant; COPD: chronic obstructive pulmonary disease; DC: dendritic cell; ExM: exudate macrophage; H&E: hematoxylin-eosin; HDM: house dust mite; iBALT: inducible bronchus-associated lymphoid tissue; IM: interstitial macrophage; mDC: myeloid dendritic cell; OVA: ovalbumin; PAS: periodic acid-Schiff stain; pDC: plasmacytoid dendritic cell.

Abstract

Asthma is a heterogeneous disease with neutrophilic and eosinophilic asthma as the main endotypes that are distinguished according to the cells recruited to the airways and the related pathology. Eosinophilic asthma is the treatment-responsive endotype, which is mainly associated with allergic asthma. Neutrophilic asthma is a treatment-resistant endotype, affecting 5-10% of asthmatics. Although eosinophilic asthma is well-studied, a clear understanding of the endotypes is essential to devise effective diagnosis and treatment approaches for neutrophilic asthma. To this end, we directly compared adjuvant-induced mouse models of neutrophilic (CFA/OVA) and eosinophilic (Alum/OVA) asthma side-by-side. The immune response in the inflamed lung was analyzed by multi-parametric flow cytometry and immunofluorescence. We found that eosinophilic asthma was characterized by a preferential recruitment of interstitial macrophages and myeloid dendritic cells, whereas in neutrophilic asthma plasmacytoid dendritic cells, exudate macrophages, and GL7^{+} activated B cells predominated. This differential distribution of macrophage and dendritic cell subsets reveals important aspects of the pathophysiology of asthma and holds the promise to be used as biomarkers to diagnose asthma endotypes.

Introduction

Asthma is a chronic airway inflammation with often debilitating impacts on the health of patients. Based on the immune cells that infiltrate into the lung, several subtypes or endotypes for asthma have been described [1–3]. Type 2-high or eosinophilic asthma is the best-understood endotype and is often triggered by inhaled antigens, like house dust mites (HDM), ragweed pollen, mold, or cockroach proteins [1,4]. This eosinophilic asthma is characterized by (i) elevated levels of eosinophils (eosinophilia) and mast cells in the bronchia, by (ii) a type 2-polarized immune response, with the production of Th2 cytokines, like IL-4, IL-5, and IL-13, and augmented production of antigen-specific IgE antibodies [1,5,6]. About half of all asthma patients have such an eosinophilic airway inflammation [1,7] and corticosteroids, anti-IgE, anti-IL-5/IL-5R, and anti-IL-4/IL-13 treatment are effective at alleviating the symptoms [1,8,9]. However, such treatment is less effective in patients with a type 2-low, neutrophil-dominated form of asthma [10,11]. This neutrophilic asthma is characterized, besides the neutrophilia, by an elevated Th1/17 immune response, indicated by the cytokines IFNγ and IL-17 [1,12–16]. Although treatments of type-2 low asthma by blocking IL-17, IL1β, or CXCR2 are in clinical trials, reports show that only a portion of the patients benefitted, suggesting the etiology of neutrophilic asthma is more complex [17].

Several *in vivo* mouse models were developed to study the pathogenic mechanisms underlying the endotypes and to develop endotype-specific treatment strategies. These mouse models differ in the means by which lung inflammation is induced. Asthma-like eosinophilic airway inflammation can be modeled by adjuvant-driven immunization [15,18–21], chronic antigen administration [19,22], and transfer of antigen-pulsed cells [18,19,23]. Asthma-like neutrophilic airway inflammation can be induced in mice by subcutaneous administration of either CFA [21,24], LPS [14,25], or poly(I:C) [26], along with a model antigen, like ovalbumin (OVA). For severe non-type 2 asthma, there is still a significant gap between disease-associated pathological features and a particular clinical outcome or treatment strategies. Hence, further research into immunological features and molecular mechanisms is required to develop new endotype-specific asthma treatments.

To determine additional immunophenotypic features specific for asthma-like neutrophilic airway inflammation, we adopted here mouse models that allowed for a direct side-by-side comparison of asthma-like eosinophilic and neutrophilic lung inflammation [15,20,21]. Specifically, we compared CFA/OVA-induced neutrophilic and Alum/OVA-induced eosinophilic asthma endotypes in mice [15,20,21] and provide an in-depth immunological analysis of the inflamed lung. Our data show that the two asthma endotypes demonstrate a significantly different distribution of macrophage and dendritic cell subsets.

Results

Adjuvant-induced mouse models of asthma endotypes

To study the immune response in the inflamed lung during eosinophilic and neutrophilic asthma side-by-side, we adopted two adjuvant-induced mouse models [15,21] (**Fig 1A**). We first confirmed that the models faithfully reflect the eosinophilic and neutrophilic asthma endotypes. As expected, the cell analysis from BALF and lung showed high levels of eosinophils (**Fig 1B**) or neutrophils (**Fig 1C**) in the eosinophilic (Alum/OVA) or neutrophilic (CFA/OVA) asthma groups, respectively. In both cases, the data from the BALF mirrored the data obtained from the lung (**Fig 1B, C**). Immunohistochemical staining of the inflamed lungs showed severe inflammation with bleeding in the neutrophilic (CFA/OVA) group (**Fig 1D**, upper panel). However, the hyper-mucus secretion, which is an important driver of the airway obstruction in asthma [1], was comparable for both endotypes (**Fig 1D**, lower panel). Furthermore, in line with the literature [27,28], the Th2 cytokines IL-5 and IL-13 were prevalent in eosinophilic asthma, whereas the Th1 cytokine IFNγ predominated in neutrophilic asthma (**Fig 1E**). Next, the antigen-specific humoral immune response was quantified. For serum IgE, higher levels were reported in eosinophilic asthma patients than in neutrophilic asthma patients [29,30], and αIgE therapy was effective for eosinophilic asthma [29,31]. However, in our mouse models, the OVA-specific serum IgE antibody levels were comparable in the eosinophilic (Alum/OVA) and neutrophilic (CFA/OVA) asthma groups (**Fig 1F**). Furthermore, and in line with clinical data [32,33], the antigen-specific serum IgG and IgG1 antibody levels were significantly higher in the eosinophilic than the neutrophilic asthma endotype (**Fig 1F**). No difference was observed for OVA-specific IgG2b and IgG2c antibody levels (**Fig 1F**). These data demonstrate that the mouse models used here successfully replicate key features of human eosinophilic and neutrophilic asthma and are suitable to investigate asthma endotypes.

Fig 1: Neutrophilic and eosinophilic asthma can successfully be modeled in mice. **(A)** Experimental design and immunization timeline. C57BL/6 mice (naïve

group n = 9 mice/group, experimental asthma groups n = 14-15 mice/group) were either immunized three times intraperitoneal (i.p.) with Alum (1 mg/mouse) for eosinophilic asthma or once subcutaneous (s.c.) with CFA (0.5 mg/mL) for neutrophilic asthma along with the model antigen OVA (20 µg/mouse). Three weeks after the first administration, the experimental groups were challenged with OVA (50 µg/mouse) daily for two days. Samples were collected 16-18 hours post-challenge. Cells from bronchoalveolar lavage fluid (BALF) and lung homogenates were stained for **(B)** eosinophils (live $CD45^+$ $CD19^-$ $CD11c^-$ $CD11b^-$ $Ly6G^-$ $Siglec\text{-}F^+$) and **(C)** neutrophils (live $CD45^+$ $CD19^-$ $CD11b^{+/lo}$ $Ly6G^+$). **(D)** H&E (upper panel) and Alcian Blue/PAS (lower panel) immunohistochemistry analysis of inflamed lungs collected from indicated groups (10X magnification, scale 127 µm). **(E)** ELISA values of IFNɣ, IL-5, and IL-13 from indicated BALF supernatants. **(F)** OVA-specific IgE, total IgG, IgG1, IgG2b, and IgG2c ELISA results in serum indicated groups (for OVA-specific antibody ELISA results, naïve group n = 3 mice/group, experimental asthma groups n = 14-15 mice/group). Combined data from three independent experiments are shown. The gating strategy for the myeloid cells is detailed in the S1 figure.

Neutrophilic asthma is characterized by high numbers of plasmacytoid dendritic cells in the BALF

We next optimized a 19-parameter flow cytometry panel to quantify myeloid cells in addition to eosinophils and neutrophils, including basophils, mast cells, monocytes, as well as dendritic cells, and macrophage subsets in the bronchoalveolar lavage fluid (BALF) and lung samples (S1 Fig). A more robust influx of leukocytes into the BALF was observed following neutrophilic (CFA/OVA) than eosinophilic (Alum/OVA) asthma, with up to 4 x 10^5 total cells/mL (**Fig 2A**). The myeloid cell populations recovered from BALF, sorted from the highest to the lowest frequency, were neutrophils/eosinophils (**Fig 1B, 1C**), monocytes, macrophages, dendritic cells (DCs) (**Fig 2A**), and few basophils (**Fig 2B**) and mast cells (**Fig 2C**). In contrast to the BALF, basophils (**Fig 2B**), and mast cells (**Fig 2C**) were found to be enriched in the lung tissue of mice with eosinophilic (Alum/OVA)

asthma. These data indicate that basophils and mast cells do not migrate to the BALF during lung inflammation. Although DCs constituted less than 1% of the BALF cells (**Fig 2A**), they were previously associated with the induction of Th2 immune responses in patients with allergic asthma [34]. To better understand the movement of DCs and their role in eosinophilic vs. neutrophilic asthma, we determined the frequency of DC subsets in the inflamed lung as $CD11b^+$ conventional (myeloid) DC (cDCs), $CD103^+$ lung resident DCs, and $CD45R^+$ plasmacytoid dendritic cells (pDCs). Both $CD11b^+$ cDC (**Fig 2D**) and lung resident $CD103^+$ DCs (**Fig 2E**) were more frequent in the lung tissue of mice with eosinophilic (Alum/OVA) than neutrophilic (CFA/OVA) asthma. In contrast, the frequency of pDCs did not change in the lung during the inflammation (**Fig 2F**). However, pDCs appeared to be the only DC population to migrate to the alveolar space, which was more prominent during neutrophilic (CFA/OVA) than eosinophilic (Alum/OVA) asthma (**Fig 2F**).

Fig 2: DC subsets, mast cells, and basophils are differentially recruited to the inflamed lungs in neutrophilic and eosinophilic asthma. C57BL/6 mice (naïve group n = 12 mice/group, experimental asthma groups n = 17-18 mice/group) were immunized as outlined in figure 1A to induce neutrophilic (CFA/OVA) or eosinophilic (Alum/OVA) asthma. Cells from bronchoalveolar lavage fluid (BALF) and lung homogenates were analyzed for indicated cell populations. **(A)** Total cell counts of all leukocytes (live $CD45^+$ cells), macrophages (live $CD19^-$ $CD45^+$ Siglec-F^- $Ly6G^-$ $F4/80^+$ $CD64^+$), dendritic cells (live $CD19^-$ $CD45^+$ Siglec-F^- $Ly6G^-$ $F4/80^-$ $CD64^-$ $CD24^+$ $CD11c^+$ MHC class $II^{+/-}$), and monocytes (live $CD19^-$ $CD45^+$ Siglec-F^- $Ly6G^-$ $F4/80^-$ $CD64^-$ $CD24^-$ $CD11c^-$ MHC class $II^{+/-}$ $Ly6C^+$) in the BALF. Total cell counts and relative cell frequencies of **(B)** basophils (live $CD45^+$ $CD19^-$ Siglec-F^- $Ly6G^-$ $CD11b^+$ $Fc\varepsilon RI\alpha^+$ $CD117^-$ cells); **(C)** mast cells (live $CD45^+$ $CD19^-$ Siglec-F^- $Ly6G^-$ $CD11b^+$ $Fc\varepsilon RI\alpha^+$ $CD117^+$ cells); **(D)** conventional DCs (cDC, live $CD45^+$ $CD19^-$ Siglec-F^- $Ly6G^-$ $CD24^+$ $CD11c^+$ MHC class II^+ $CD103^-$ $CD11b^+$ cells); **(E)** $CD103^+$ DCs (live $CD45^+$ $CD19^-$ Siglec-F^- $Ly6G^-$ $CD24^+$ $CD11c^+$ MHC class II^+ $CD103^+$ cells); and **(F)** plasmacytoid dendritic cells (pDC, live $CD19^-$ $CD45^+$ Siglec-F^- $Ly6G^-$ $CD11b^-$ $CD45R^+$ $Ly6C^+$) in indicated organs. Combined data from four (A, D-F) or three (B, C) independent experiments are shown.

The frequency of exudate and interstitial macrophages markedly differs between asthma endotypes

In the steady-state, pulmonary macrophages consist mainly of two subsets, alveolar macrophages (AMs) and interstitial macrophages (IMs) [35]. AMs, which represent the major portion of lung resident macrophages, are tissue-resident macrophages of embryonic origin that self-renew in the lung [36,37]. In contrast, IMs are derived from blood monocytes that infiltrated into the lung parenchyma [37,38]. During lung inflammations, another blood monocyte-derived macrophage population that can be found in the lung are the non-resident Ly6C^{hi} or exudate macrophages (ExMs) [39–42]. To characterize the turnover of macrophages in the two asthma endotypes, the frequency of AMs, IMs, and ExMs was determined in the BALF and lungs. In line with the large increase of macrophages in the lung (Figure 2A), the frequency of AMs considerably declined in the BALF and the lung of both asthma groups compared to the control group (**Fig 3A**). As IMs are located mainly in the lung parenchyma [37], it was expected that their numbers did not greatly increase in the BALF, leading to a sharp decline in their relative frequency in the BALF (**Fig 3B**). Interestingly, however, an increase in the frequency of IMs in the lung was only observed in the mice with eosinophilic (Alum/OVA) and not neutrophilic (CFA/OVA) asthma (**Fig 3B**). In contrast, the influx of ExMs was more prominent in the neutrophilic (CFA/OVA) than the eosinophilic (Alum/OVA) asthma group, which was particularly striking in the BALF (**Fig 3C**). Recently, it was suggested that the IMs themselves can be divided into three subsets, based on the expression of CD11b, CD11c, and MHC class II [38]. When these subsets were analyzed (**Fig 3D-F**), we noticed that the IM population in the eosinophilic (Alum/OVA) inflammation mainly consisted of the CD11c^{+} MHC class II^{neg} population (**Fig 3E, F**), which was described to have the highest phagocytic activity and the lowest turnover rate among the IM subsets [38]. Together, these data indicate that eosinophilic and neutrophilic asthma involve significantly different macrophage populations, with IMs increasing in the lungs with eosinophilic asthma and ExMs increasing in neutrophilic asthma.

Fig 3: The distribution of lung macrophage subsets among asthma endotypes. C57BL/6 mice (naïve group n = 12 mice/group, experimental asthma groups n = 17-18 mice/group) were immunized as outlined in figure 1A to induce neutrophilic (CFA/OVA) or eosinophilic (Alum/OVA) asthma. Cells from bronchoalveolar lavage fluid (BALF) and lung homogenates were analyzed for indicated cell populations: **(A)** alveolar macrophages (AMs, live $CD45^+$ $CD19^-$ Siglec-F^+ $Ly6G^-$ $CD11c^+$ cells), **(B)** interstitial macrophages (IMs, live $CD45^+$ $CD19^-$ Siglec-F^- $Ly6G^-$ $CD24^-$ $F4/80^+$ $CD64^{+/-}$ $Ly6C^-$ $CD11b^+$ cells); and **(C)** exudate macrophages (ExMs, live $CD45^+$ $CD19^-$ Siglec-F^- $Ly6G^-$ $CD24^-$ $F4/80^+$ $CD64^{+/-}$ $Ly6C^+$ $CD11b^+$ cells). **(D)** Representative dot plots showing IMs ($Ly6C^-$ $CD11b^+$ cells) and ExMs ($Ly6C^+$ $CD11b^+$ cells) in BALF (upper panel) and lung (lower panel) from indicated groups. **(E)** Representative histograms showing the expression of MHC class II, CD11b, and CD11c on bronchial IMs from indicated groups. **(F)** Bronchial IMs (BIMs) were subdivided according to their expression of CD11c and MHC class II and the frequencies of BIM1 ($CD11c^+$ MHC class II^+, left panel), BIM2 ($CD11c^-$ MHC class II^+, middle panel), and BIM3 ($CD11c^+$ MHC class II^{neg}, right panel) cells are shown. Combined data from four independent experiments are shown.

Th17 cells, but not NKT17 cells, are significantly expanded in neutrophilic asthma

Both conventional $CD4^+$ T cells [43,44] and innate-like invariant Natural Killer (*i*NKT) cells [45–48] have been shown to be involved in asthma in humans and mouse models. Therefore, we next measured the subset distributions of $CD4^+$ T cells (Th1, Th2, Th17, Treg) and *i*NKT cells (NKT1, NKT2, NKT17) in our eosinophilic and neutrophilic asthma model. Surprisingly, for the frequency of Th1 and Th2 cells and of Tregs, no significant difference was observed in the lungs of mice with eosinophilic (Alum/OVA) or neutrophilic (CFA/OVA) asthma (**Fig 4A**). Similarly, the production of the cytokines IFNγ, IL-4, IL-13, and TNF by $CD4^+$ T cells did not differ between the eosinophilic (Alum/OVA) and neutrophilic (CFA/OVA) asthma groups (**Fig 4B**). In contrast, the frequency of Th17 cells

in the lung (**Fig 4A**), as well as the production of IL-17 by $CD4^+$ T cells (**Fig 4B**), was significantly higher in the lungs of mice with neutrophilic (CFA/OVA) than with eosinophilic (Alum/OVA) asthma. The lung *i*NKT cells (**Fig 4C**) were mainly NKT1 cells (**Fig 4D**) and their frequency increased during neutrophilic (CFA/OVA) asthma (**Fig 4D**). No changes were observed in the lungs for NKT2 cells (**Fig 4D**). However, the frequency of NKT17 cells decreased during neutrophilic (CFA/OVA) asthma (**Fig 4D**), which was, interestingly, the opposite of the changes observed for Th17 cells (**Fig 4A**).

Fig 4: Frequency of $CD4^+$ T and *i*NKT cell subsets in the inflamed lungs during neutrophilic and eosinophilic asthma. C57BL/6 mice (naïve group n = 12 mice/group, experimental asthma groups n = 17-18 mice/group) were immunized as outlined in figure 1A to induce neutrophilic (CFA/OVA) or eosinophilic (Alum/OVA) asthma. Cells from lung homogenates were stained for indicated cell populations. **(A)** The relative cell frequency of lung Th1 cells (live $CD19^-$ $CD3\varepsilon^+$ $CD4^+$ $FoxP3^-$ $Tbet^+$ cells), Th2 cells (live $CD19^-$ $CD3\varepsilon^+$ $CD4^+$ $FoxP3^-$ $Gata3^+$ cells), Th17 cells (live $CD19^-$ $CD3\varepsilon^+$ $CD4^+$ $FoxP3^-$ $ROR\gamma t^+$ cells), and Tregs (live $CD19^-$ $CD3\varepsilon^+$ $CD4^+$ $CD127^{lo/-}$ $FoxP3^+$ cells) is shown. **(B)** Production of the indicated cytokines by lung $CD4^+$ T cells following *in vitro* stimulation with PMA and ionomycin. **(C)** Gating for *i*NKT cell (live $CD19^-$ $CD3\varepsilon^+$ CD1d/PBS57-$tetramer^+$ cells) subsets in the lung (NKT1 cells: $PLZF^{lo}$ $ROR\gamma t^-$ cells, NKT2 cells: $PLZF^{int/hi}$ $ROR\gamma t^-$ cells, NKT17 cells: $PLZF^{int}$ $ROR\gamma t^+$ cells). **(D)** Relative frequency of NKT1 and NKT17 cells in the lung of indicated mice. Combined data from three (C, D), four (A), or two (B) independent experiments are shown. The gating strategy for the lymphoid cells is detailed in the S2 figure.

Neutrophilic asthma is characterized by an increase of activated B cell numbers

B cells, besides their ability to produce allergen-specific antibodies [49], are involved in the pathogenesis of chronic lung inflammation either by presenting antigens to T cells

[50] or by the formation of 'inducible bronchus-associated lymphoid tissue' (iBALTs) [51]. iBALTs are tertiary lymphoid structures that are rapidly induced and provide an effective local site to drive lymphocyte activation and immune response in the lung [52]. To assess the B cell responses during eosinophilic (Alum/OVA) and neutrophilic (CFA/OVA) asthma, we measured the frequency of B cells and their cytokine production, as well as the frequency of germinal center (GC) B cells in the lungs. Although the overall frequency of B cell was comparable between the BALFs and lungs with eosinophilic (Alum/OVA) or neutrophilic (CFA/OVA) asthma (**Fig 5A**), the IFNγ production of B cells from lungs with neutrophilic asthma was significantly higher than in the neutrophilic asthma group (**Fig 5B**). No difference was observed for IL-4, IL-17, and TNF production by the B cells (**Fig 5B**). Importantly, we noticed a significant increase of CD45R/B220$^+$ GL7$^+$ CD95$^+$ germinal center (GC) B cells in the lungs of mice with neutrophilic (CFA/OVA) asthma, which was not observed in the lungs from mice with eosinophilic (Alum/OVA) asthma (**Fig 5C**). These data indicate that iBALT formation was only supported during neutrophilic asthma in our mouse models, a finding that was supported by the immunofluorescence of the inflamed lungs (**Fig 5D**).

Fig 5: iBALT formation is more pronounced in neutrophilic than in eosinophilic asthma. C57BL/6 mice (naïve group n = 5 mice/group, experimental asthma groups n = 8-9 mice/group) were immunized as outlined in figure 1A to induce neutrophilic (CFA/OVA) or eosinophilic (Alum/OVA) asthma. Cells from bronchoalveolar lavage fluid (BALF) and lung homogenates were analyzed for indicated cell populations. (**A)** Total cell count (left panel) and relative cell frequencies of B cells (live CD45$^+$) in indicated organs. **(B)** Production of the indicated cytokines by lung B cells (live CD45$^+$) following *in vitro* stimulation with PMA and ionomycin. The values are given as fold-change of the two experimental groups over the control group. **(C)** Relative cell frequencies of germinal center (GC) B cells (live CD3ε^- CD45R$^+$ CD95$^+$ GL7$^+$ cells) in lung homogenates. **(D)** Inflamed lungs were fixed with 4% PFA (4h, 4°C), prepared for cryostat sectioning (7-10 µm), and stained with DAPI (white), CD45R-AF647 (blue), GL7-AF488

(green), and TCRβ-AF594 (red). Scale = 50 μm. Representative data from three biological replicates are shown. Unless indicated otherwise, combined data from two independent experiments are shown.

Discussion

Neutrophilic asthma responds poorly to the main treatment options currently available for asthma patients, severely impacting the quality of life of patients. A better understanding of the immunological features and underlying immunopathology of the different asthma endotypes is expected to lead the way to improved therapies. Here, we directly compared in detail the immune response (i) between asthma-like neutrophilic airway inflammation in mouse models and (ii) between BALF vs. lung tissue of those mice. Our data demonstrate that the BALF provides a good immunological representation of the inflamed lung. Furthermore, asthma endotypes are characterized by the distinct distribution of several myeloid cells, besides eosinophils and neutrophils; namely cDCs, $CD103^+$ DCs, pDCs, interstitial macrophages (IMs), and exudate macrophages (ExMs). For these populations, several differences between BALF and lung tissue were noted, which indicates that pDCs and ExMs in BALF can identify neutrophilic asthma in mice. Furthermore, Th17 cells, but not NKT17 cells or germinal center B cells, were significantly expanded in neutrophilic asthma.

Asthma is a heterogeneous disease and new endotypes are being described in the clinic. However, many challenges remain. Airway inflammations, like asthma, have long been modeled *in vivo* in animals to gain insight into pathogenesis, progression, and treatment options. Despite their intrinsic limitations, such animal models are instrumental for our understanding of complex human diseases. Prime/boost immunization of mice with ovalbumin (OVA) together with the adjuvant Alum (aluminum hydroxide) is a well-described approach to induce a type-2 immune response in the airways, including antigen-specific IgEs, hypersensitivity responses, and airway remodeling [32]. Clinically relevant allergens, such as extracts of house dust mites (HDM), have also been used in animal models [53,54]. However, their use is hampered by technical difficulties and a lack of standardization, which reduces reproducibility [55]. For neutrophilic asthma, less work and fewer animal models have been reported [56]. Based on literature data and our preliminary results, we concluded that the adjuvant-induced eosinophilic (Alum/OVA) and neutrophilic (CFA/OVA) asthma models used here are best suited to compare asthma-like eosinophilic and neutrophilic lung inflammation side-by-side.

Basophils [57,58] and mast cells [59,60] are associated with allergen-induced airway inflammation due to IgE-mediated effector functions. In line with these reports, we noted a clear increase in basophils (Fig 2B) and mast cells (Fig 2C) in the lungs of mice with eosinophilic airway inflammation (Alum/OVA). Furthermore, our data indicate that basophils and mast cells do not migrate to the BALF during allergen-induced lung inflammation. To our knowledge, this is the first report showing this directly for eosinophilic and neutrophilic asthma. In Th2-low (neutrophilic) asthma, mast cells locate to the proximal airway epithelium [61,62] and the submucosal region [63], whereas in Th2-high (eosinophilic) asthma, they are found in the intraepithelial region [61,62]. Therefore, it seems possible that the location of the mast cells, and potentially the basophils, in the inflamed lung limits their propensity to migrate to the BALF.

In allergic, eosinophilic airway inflammation, the antigen presentation by pulmonary $CD11b^+$ cDCs and $CD103^+$ cDCs is essential for the induction of the Th2 response [64]. Although pDCs have the ability, similar to other pulmonary DCs, to take up and process antigens [65], they actually prevent the differentiation of effector T cells, and depletion of pDCs could exacerbate lung inflammation in an LPS-induced asthma model [66,67]. In addition, pDCs are associated with the induction of type 1 immune responses and, for example, protect from viral bronchiolitis [68] and suppress ILC2 activity via IFNα during fungus-induced allergic asthma [69]. Similar to the literature, we found that conventional pulmonary DCs, including $CD11b^+$ and $CD103^+$ cDCs, are significantly expanded in eosinophilic asthma (Fig 2D, 2E). In contrast, in neutrophilic asthma, pDCs were the only DCs that infiltrated the alveolar space of the inflamed lung (Fig 2F). Although pDCs have been reported to increase upon allergen challenge in the BALF [70] and the induced sputum [71] of asthmatic patients, to our knowledge, no study compared their frequency in different endotypes. Interestingly, the increase of pDCs in the BALF was not accompanied by an increase of pDCs in the lung itself (Fig 2F).

Macrophages are important innate immune cells involved in tissue homeostasis and host defense. Lung macrophage subsets were initially defined by their location: alveolar macrophages (AMs) are mainly found in the alveolar lumen, whereas interstitial macrophages (IMs) reside in the lung interstitium [35,72]. AMs are essential for the repair of lung injuries induced, e.g. by physical damage [73], LPS [74,75], or infections [39].

Consequently, AMs are also protective during allergic airway inflammation [76] and lung fibrosis [77]. In contrast, IMs, which constitute approx. 9% of the macrophages in a healthy lung [38], have primarily proinflammatory functions. For example, they aggravate allergic inflammation [78] and fibrosis [79]. During lung inflammations, blood-monocytes can infiltrate the lung and give rise to a third lung macrophage population, Ly6C^{hi} exudate macrophages (ExMs). ExMs are mainly proinflammatory and have been described, for example, during lung inflammations caused by diphtheria toxin [41] and infections with bacteria [39,42], fungi [40], or viruses [80]. Due to their functional differences, it is important to analyze macrophages on the subset level during pulmonary diseases. When we analyzed AMs, IMs, and ExMs from the BALF and the inflamed lung of mice with eosinophilic and neutrophilic asthma, several changes were apparent. In line with previous findings [81], AMs significantly declined during both types of lung inflammation (Fig 3A). Importantly, we found that the frequency of IMs and ExMs distinguishes the two asthma endotypes, with IMs being expanded more in eosinophilic asthma (Fig 3B) and ExMs being more prevalent in neutrophilic asthma (Fig 3C). Further analysis of the IMs based on surface markers [38], showed that the IMs in both endotypes mainly consisted of the CD11c^{lo} MHC class II^{neg} population (Fig 3E, F), which has high phagocytic activity [38]. It will be important to clarify if the differences in the distribution of macrophage populations can be used as biomarkers to stratify asthma patients.

Analyzing T cells, we noted the increase of Th17 cells and IL-17 production in neutrophilic asthma (Fig 4A, B), which is in line with previous reports [82]. In contrast to the Th17 cells, however, the frequency of NKT17 cells was decreased in neutrophilic asthma (Fig 4D), suggesting that *i*NKT cells might be less relevant for the pathology of this asthma endotype.

iBALTs (inducible bronchus-associated lymphoid tissues) are tertiary lymphoid tissue, structurally similar to germinal centers in the lymph nodes, which are formed in the airways during lung inflammation, for example, following infections or during chronic diseases, like COPD (chronic obstructive pulmonary disease) [52]. In allergic asthma models, iBALTs support the Th2 cell responses induced by fungal infection [83] or LPS [84]. Within iBALTs, germinal center (GC) B cells can act as APCs by presenting inhaled antigens to T cells and can drive their differentiation into Th2 cells [50]. Conversely,

antigen-specific Th2 cells can support iBALT formation [85]. However, the role of iBALT in neutrophilic asthma and how it would compare to eosinophilic asthma is not known. We provide here, to our knowledge, the first direct comparison of GC B cells and iBALTs in these two asthma endotypes. Histological examination did not indicate that the size of the iBALTs differed between the two endotypes (Fig 5D). However, we found that in neutrophilic but not eosinophilic asthma the frequency of GC B cells was greatly increased (Fig 5C) and that they produce more IFNγ following activation (Fig 5B). These data suggest that activated B cells, locally in the inflamed lung, might contribute to the pathology in neutrophilic asthma.

Our side-by-side comparison of BALF and lung tissue also revealed several unexpected discrepancies. Although we observed clear differences between eosinophilic and neutrophilic asthma in the lungs for basophils, mast cells, cDCs, CD103$^+$ DCs (Fig 2B-E), as well as IMs (Fig 3B), these changes were not represented in the BALF. As BALF of asthma patients is easier accessible than lung tissue, it is important to know which cell populations in the BALF are most indicative for the lung inflammation. Our data indicate that both pDCs (Fig 2F) and ExMs (Fig 3C) were markedly increased in the BALF of mice with neutrophilic but not eosinophilic asthma, making them possible candidates for the clinical diagnosis of asthma endotypes.

In summary, we report here, to our knowledge for the first time, a direct side-by-side comparison of the main myeloid cell populations, *i*NKT cells, and GC B cells from the inflamed lungs of mice with adjuvant-induced eosinophilic and neutrophilic asthma. These data suggest that the subset distribution of macrophages and dendritic cells in the BALF could be used to aid the determination of asthma endotypes. Although further research is required to verify these results in asthma patients, the differential distribution of myeloid cells, other than eosinophils and neutrophils, promises to be helpful as an early biomarker to support the stratification of asthma endotypes.

Material and Methods

Mice

All mice were housed in the vivarium of the Izmir Biomedicine and Genome Center (IBG, Izmir, Turkey) in accordance with the respective institutional animal care committee guidelines. All mouse experiments were performed with prior approval by the institutional ethic committee ('Ethical Committee on Animal Experimentation'), in accordance with national laws and policies. All the methods were carried out in accordance with the approved guidelines and regulations.

Reagents, monoclonal antibodies, and flow cytometry

Monoclonal antibodies against the following mouse antigens were used in this study: CD3ε (145.2C11, 17A2), CD4 (RM4-5), CD8α (53-6.7, 5H10), CD11b (M1/70), CD11c (N418), CD19 (1D3, 6D5), CD24 (M1/69), CD44 (IM7), CD45 (30-F11), CD45.2 (104) CD45R/B220 (RA3-6B2), CD64 (X54-5/7.1), CD95 (SA367H8), CD103 (3E7), CD117/cKit (2B8), CD122 (TM-beta1), CD127 (A7R34, SB/199), CD170/Siglec F (E50-2440), F4/80 (BM8), FcεRIα (MAR-1), FoxP3 (FJK-16s), Gata3 (L50-823), GL7 (GL7), IFNγ (XMG1.2), IL-4 (11B11), IL-13 (13A), IL-17A (TC11-18H10), Ly6G (1A8), Ly6C (HK1.4), MHC class II (M5/114.15.2), NK1.1 (PK136), PLZF (9E12), RORγt (Q31-378), Tbet (O4-46), TCRβ (H57-597), TNF (MP6-XT22). Antibodies were purchased from BD Biosciences (San Diego, CA), BioLegend (San Diego, CA), eBioscience (San Diego, CA), or ThermoFisher Scientific (Carlsbad, CA). Antibodies were biotinylated or conjugated to Pacific Blue, eFluor 450, Brilliant Violet 421, V500, Brilliant Violet 510, Brilliant Violet 570, Brilliant Violet 650, Brilliant Violet 711, Brilliant Violet 785, Brilliant Violet 786, FITC, Alexa Fluor 488, PerCP-Cy5.5, PerCP-eFluor 710, PE, PE-CF594, PE-Cy7, APC, Alexa Fluor 647, eFluor 660, Alexa Fluor 700, APC-Cy7, APC-eFluor 780 or APC-Fire750. Anti-mouse CD16/32 antibody (2.4G2) used for Fc receptor blocking was obtained from Tonbo Biosciences. Unconjugated mouse and rat IgG antibodies were purchase from Jackson ImmunoResearch (West Grove, PA). Dead cells were labeled with Zombie UV Dead Cell

Staining Kit (BioLegend). Flow cytometry was performed as described [86]. Graphs derived from digital data are displayed using a 'bi-exponential display' [87]. The gating strategy utilized is outlined in the S1 and S2 figures.

Adjuvant-induced asthma models

Neutrophilic asthma was induced by one injection (d0) per mouse with 0.5 mg/mL CFA (Complete Freund's Adjuvant, Sigma-Aldrich, St. Louis, MO) mixed with 20 µg OVA (Ovalbumin, Hyglos, Germany) [15,21]. Eosinophilic asthma was induced by weekly injections (d0, d7, d14) per mouse of 1 mg Alum ('Imject Alum', ThermoFisher Scientific) mixed with 20 µg OVA [15,21]. Seven days after the last Alum/OVA injection, all mice were challenged with 50 µg OVA/mouse by pharyngeal/laryngeal installation once on two consecutive days (d21, d22). 16-18 hours later, the mice were sacrificed, and the blood, BALFs, and lungs were collected to assess immune responses by flow cytometry, ELISA, and immunohistochemistry/immunofluorescence.

Cell preparation

Bronchoalveolar lavage fluid (BALF) was collected by inflating the murine lungs with 1 mL ice-cold PBS, which was repeated twice with fresh PBS. The three washes were centrifugated separately at 400 *g* for 7 min at 4°C. The supernatant of the first wash was collected for the ELISA analysis, the cells of all three washes were pooled for the flow cytometric analysis. Single-cell suspensions from mouse lungs were prepared as described [88]. In brief, lungs were removed and minced into smaller pieces in a 6-well plate (Greiner, Germany). The digestion mixture, composed of 1 mg/mL collagenase D and 0.1 mg/mL DNase I (both from Roche, Switzerland) in complete RPMI medium (Gibco, USA), was added to the samples and incubated for 30 min at 37°C on a lateral shaker. The lung samples were filtered through 100 µm mesh with PBS, washed twice, and the red blood cells were eliminated by ACK lysis buffer (Lonza, US).

ELISA

The IFNɣ, IL-5, and IL-13 cytokine levels in BALF were measured with the respective Sandwich-ELISA kits (R&D Systems, MN, US) according to the manufacturer's instructions. OVA-specific antibodies were measured in the sera, collected from mice via cardiac puncture, as described [89]. For detecting total IgG, IgG1, IgG2, and IgA antibodies, the sera were serial diluted and loaded onto 10 µg OVA-coated plates. Horseradish peroxidase (HRP)-conjugated anti-mouse IgG, IgG1, IgG2, IgA (Southern Biotech, USA) antibodies were used as detection antibodies. For the detection of OVA-specific IgE antibodies, the sera were diluted 1/10 with PBS containing 1% (w/v) BSA and loaded onto anti-mouse IgE coated (BD biosciences) plates anti-OVA-HRP antibodies (AbD Serotec, BioRad) were used as detection antibody [89]. The colorimetric change, resulting from the enzymatic reaction between the HRP portion of detection antibody and the substrate TMB, was measured as absorbance at 450 nm (OD450) by Spectrophotometer (Thermo Scientific, Multiskan FC Microplate Photometer). The titers were defined from the reciprocal value of the absorbance at OD450.

In vitro stimulation

Lung-derived lymphocytes were stimulated *in vitro* with PMA (50 ng/mL) and ionomycin (1 µg/mL) (both Sigma-Aldrich, St. Louis, MO) for four hours at 37°C in the presence of both Brefeldin A (GolgiPlug) and Monensin (GolgiStop). As GolgiPlug and GolgiStop (both BD Biosciences, San Diego, CA) were used together, half the amount recommended by the manufacturer were used, as suggested previously [90].

Histology

Lungs were inflated with 4% PFA (Cell Signaling, San Diego, US) and fixed for four hours on a lateral shaker at 4°C. After dehydration with 30% sucrose overnight on a lateral shaker at 4°C, samples were embedded in O.C.T (Tissue Tek, Sakura, US) and snap-frozen. 7-10 µm thick sections were prepared with a cryostat (Leica CM 1950). For the H&E staining, the tissue sections were stained with hematoxylin (Sigma, USA) and eosin

(Sigma, USA) for two minutes each. Slide contrast was increased by a brief HCl/ethanol treatment (1/1000, v/v) (Sigma, USA). Slides were fixed by ascending concentration of ethanol (70%, 80%, 90%, 95%, 100%) (Sigma, USA) and a final 5 second xylene (Sigma, USA) treatment. For the Alcian Blue/PAS staining, the tissue sections were stained with an Alcian Blue/PAS staining kit according to the manufacturer's recommendations (Bio Optica, Italy). Once the slides dried, they were mounted with entellan and examined with a light microscope (Olympus IX71). For the immunofluorescence, tissue sections were stained with CD45R-AF647 (BD Biosciences, San Diego, CA, US) and DAPI (ThermoFisher Scientific, Carlsbad, CA) and analyzed with a confocal microscope (Zeiss LSM 880).

Statistical analysis

Data are presented as mean ± standard error of the mean (SEM). The statistical analysis was performed with GraphPad Prism 7.0 software (GraphPad Software, San Diego, CA). One-way ANOVA followed by Holm-Sidak posthoc test are used to compare p values regarded as *$p \leq 0.05$, **$p \leq 0.01$, and ***$p \leq 0.001$.

Acknowledgments

The authors wish to thank the Flow Cytometry Core Facility, Histopathology Core Facility, Imaging Core Facility, and the vivarium at the Izmir Biomedicine and Genome Center (IBG) for technical assistance. We are grateful to the NIH Tetramer Core Facility for providing the PBS57-loaded mouse CD1d tetramers and to Dr. Duygu Sag for critical reading of the manuscript.

Author Contributions

Conceived and designed the experiments: MO, GW. Performed the experiments and analyzed the data: MO, YCE. Wrote the paper: MO, GW. All authors reviewed and approved the manuscript.

Competing financial interests

The authors have declared that no competing interests exist.

References

1. Global initiative for Asthma. Global Strategy for Asthma Management and Prevention, available from www.ginasthma.org. 2020.
2. Agache I, Akdis C, Jutel M, Virchow JC. Untangling asthma phenotypes and endotypes. Vol. 67, Allergy: European Journal of Allergy and Clinical Immunology. 2012. p. 835–46.
3. Simpson JL, Grissell T V., Douwes J, Scott RJ, Boyle MJ, Gibson PG. Innate immune activation in neutrophilic asthma and bronchiectasis. Thorax. 2007;62(3):211–8.
4. Lambrecht BN, Hammad H. The immunology of asthma. Nat Immunol. 2015;16(1):45–56.
5. Peters MC, Mekonnen ZK, Yuan S, Bhakta NR, Woodruff PG, Fahy J V. Measures of gene expression in sputum cells can identify T H2-high and TH2-low subtypes of asthma. J Allergy Clin Immunol. 2014;133(2). Available from: http://dx.doi.org/10.1016/j.jaci.2013.07.036
6. Hodge S, Hodge G, Simpson JL, Yang IA, Upham J, James A, et al. Blood cytotoxic/inflammatory mediators in non-eosinophilic asthma. Clin Exp Allergy. 2016;46(1):60–70.
7. McGrath KW, Icitovic N, Boushey HA, Lazarus SC, Sutherland ER, Chinchilli VM, et al. A large subgroup of mild-to-moderate asthma is persistently noneosinophilic. Am J Respir Crit Care Med. 2012;185(6):612–9.
8. Pavord ID, Beasley R, Agusti A, Anderson GP, Bel E, Brusselle G, et al. After asthma: redefining airways diseases. Lancet. 2018;391(10118):350–400. Available from: http://dx.doi.org/10.1016/S0140-6736(17)30879-6
9. Samitas K, Delimpoura V, Zervas E, Gaga M. Anti-IgE treatment, airway inflammation and remodelling in severe allergic asthma: Current knowledge and future perspectives. Eur Respir Rev. 2015;24(138):594–601. Available from: http://dx.doi.org/10.1183/16000617.00001715
10. Gibson PG, Simpson JL, Saltos N. Heterogeneity of airway inflammation in persistent

562 asthma: Evidence of neutrophilic inflammation and increased sputum interleukin-8.
563 Chest. 2001;119(5):1329–36. Available from:
564 http://dx.doi.org/10.1378/chest.119.5.1329

565 11. McGrath KW, Icitovic N, Boushey HA, Lazarus SC, Sutherland ER, Chinchilli VM, et
566 al. A large subgroup of mild-to-moderate asthma is persistently noneosinophilic. Am
567 J Respir Crit Care Med. 2012;185(6):612–9.

568 12. Wadhwa R, Dua K, Adcock IM, Horvat JC, Kim RY, Hansbro PM. Cellular
569 mechanisms underlying steroid-resistant asthma. Eur Respir Rev. 2019;28(153):1–
570 10. Available from: http://dx.doi.org/10.1183/16000617.0096-2019

571 13. Sze E, Bhalla A, Nair P. Mechanisms and therapeutic strategies for non-T2 asthma.
572 Allergy Eur J Allergy Clin Immunol. 2020;75(2):311–25.

573 14. Whitehead GS, Thomas SY, Cook DN. Modulation of distinct asthmatic phenotypes
574 in mice by dose-dependent inhalation of microbial products. Environ Health Perspect.
575 2014;122(1):34–42.

576 15. Dejager L, Dendoncker K, Eggermont M, Souffriau J, Van Hauwermeiren F, Willart
577 M, et al. Neutralizing TNFα restores glucocorticoid sensitivity in a mouse model of
578 neutrophilic airway inflammation. Mucosal Immunol . 2015;8(January):1–14.
579 Available from: http://www.nature.com/doifinder/10.1038/mi.2015.12

580 16. Mcalees JW, Whitehead GS, Harley ITW, Cappelletti M, Rewerts CL, Holdcroft AM,
581 et al. Distinct Tlr4 -expressing cell compartments control neutrophilic and eosinophilic
582 airway inflammation. 2014;8(4):863–73. Available from:
583 http://dx.doi.org/10.1038/mi.2014.117

584 17. Kalchiem-Dekel O, Yao X, Levine SJ. Meeting the Challenge of Identifying New
585 Treatments for Type 2-Low Neutrophilic Asthma. Chest . 2020;157(1):26–33.
586 Available from: https://doi.org/10.1016/j.chest.2019.08.2192

587 18. Kips JC, Anderson GP, Fredberg JJ, Herz U, Inman MD, Jordana M, et al. Murine
588 models of asthma. Eur Respir J. 2003;22(2):374–82.

589 19. Yu QL, Chen Z. Establishment of different experimental asthma models in mice. Exp
590 Ther Med. 2018;15(3):2492–8.

591 20. Jang E, Nguyen QT, Kim S, Kim D, Le THN, Keslar K, et al. Lung-Infiltrating Foxp3 +
592 Regulatory T Cells Are Quantitatively and Qualitatively Different during Eosinophilic
593 and Neutrophilic Allergic Airway Inflammation but Essential To Control the
594 Inflammation. J Immunol. 2017;199(12):3943–51.

595 21. Bogaert P, Naessens T, de Koker S, Hennuy B, Hacha J, Smet M, et al. Inflammatory
596 signatures for eosinophilic vs. neutrophilic allergic pulmonary inflammation reveal
597 critical regulatory checkpoints. Am J Physiol - Lung Cell Mol Physiol.
598 2011;300(5):679–90.

599 22. Haspeslagh E, Debeuf N, Hammad H, Lambrecht BN. Murine models of allergic
600 asthma. Methods Mol Biol. 2017;1559:121–36.

601 23. Hayashi N, Yoshimoto T, Izuhara K, Matsui K, Tanaka T, Nakanishi K. T helper 1
602 cells stimulated with ovalbumin and IL-18 induce airway hyperresponsiveness and
603 lung fibrosis by IFN-γ and IL-13 production. Proc Natl Acad Sci U S A.
604 2007;104(37):14765–70.

605 24. Dejager L, Dendoncker K, Eggermont M, Souffriau J, Van Hauwermeiren F, Willart
606 M, et al. Neutralizing TNFα restores glucocorticoid sensitivity in a mouse model of
607 neutrophilic airway inflammation. Mucosal Immunol . 2015;8(January):1–14.
608 Available from: http://dx.doi.org/10.1038/mi.2015.12

609 25. Wilson RH, Whitehead GS, Nakano H, Free ME, Kolls JK, Cook DN. Allergic
610 Sensitization through the Airway Primes Th17-dependent Neutrophilia and Airway
611 Hyperresponsiveness.

612 26. Sadamatsu H, Takahashi K, Tashiro H, Kato G, Noguchi Y, Kurata K, et al. The non-
613 antibiotic macrolide EM900 attenuates HDM and poly(I:C)-induced airway
614 inflammation with inhibition of macrophages in a mouse model. Inflamm Res.
615 2020;69(1):139–51.

616 27. Edwards MR, Saglani S, Schwarze J, Skevaki C, Smith JA, Ainsworth B, et al.
617 Addressing unmet needs in understanding asthma mechanisms . Vol. 49, European
618 Respiratory Journal. 2017. Available from:
619 http://dx.doi.org/10.1183/13993003.02448-2016

620 28. Agache I, Cojanu C, Rogozea L. Endotype-driven approach for asthma. Implement
621 Precis Med Best Pract Chronic Airw Dis. 2018;45–9.

622 29. Wu W, Bleecker E, Moore W, Busse WW, Castro M, Chung KF, et al. Unsupervised
623 phenotyping of Severe Asthma Research Program participants using expanded lung
624 data. J Allergy Clin Immunol . 2014;133(5):1280–8. Available from:
625 http://dx.doi.org/10.1016/j.jaci.2013.11.042

626 30. Ray A, Kolls JK. Neutrophilic Inflammation in Asthma and Association with Disease
627 Severity. Trends Immunol . 2017;xx:1–13. Available from:
628 http://dx.doi.org/10.1016/j.it.2017.07.003

629 31. Huang YC, Weng CM, Lee MJ, Lin SM, Wang CH, Kuo HP. Endotypes of severe
630 allergic asthma patients who clinically benefit from anti-IgE therapy. Clin Exp Allergy.
631 2019;49(1):44–53.

632 32. Ray A, Kolls JK. Neutrophilic Inflammation in Asthma and Association with Disease
633 Severity. Trends Immunol . 2017;38(12):942–54. Available from:
634 http://dx.doi.org/10.1016/j.it.2017.07.003

635 33. Verduyn M, Botto G, Jaubert J, Lier C, Flament T, Guilleminault L. Serum IgG
636 Concentrations in Adult Patients Experiencing Virus-Induced Severe Asthma
637 Exacerbations. J Allergy Clin Immunol Pract. 2019;7(5):1507-1513.e1.

638 34. Upham JW, Denburg JA, O'Byrne PM. Rapid response of circulating myeloid dendritic
639 cells to inhaled allergen in asthmatic subjects. Clin Exp Allergy. 2002;32(6):818–23.

640 35. Byrne AJ, Maher TM, Lloyd CM. Pulmonary Macrophages: A New Therapeutic
641 Pathway in Fibrosing Lung Disease? Trends Mol Med . 2016;22(4):303–16. Available
642 from: http://dx.doi.org/10.1016/j.molmed.2016.02.004

643 36. Ginhoux F, Guilliams M. Tissue-Resident Macrophage Ontogeny and Homeostasis.
644 Immunity . 2016;44(3):439–49. Available from:
645 http://dx.doi.org/10.1016/j.immuni.2016.02.024

646 37. Evren E, Ringqvist E, Willinger T. Origin and ontogeny of lung macrophages: from
647 mice to humans. Immunology. 2020;160(2):126–38.

648 38. Gibbings SL, Thomas SM, Atif SM, McCubbrey AL, Desch AN, Danhorn T, et al.

649 Three unique interstitial macrophages in the murine lung at steady state. Am J Respir
650 Cell Mol Biol. 2017;57(1):66–76.

651 39. Taut K, Winter C, Briles DE, Paton JC, Christman JW, Maus R, et al. Macrophage
652 turnover kinetics in the lungs of mice infected with Streptococcus pneumoniae. Am J
653 Respir Cell Mol Biol. 2008;38(1):105–13.

654 40. Osterholzer JJ, Chen GH, Olszewski MA, Zhang YM, Curtis JL, Huffnagle GB, et al.
655 Chemokine receptor 2-mediated accumulation of fungicidal exudate macrophages in
656 mice that clear cryptococcal lung infection. Am J Pathol . 2011;178(1):198–211.
657 Available from: http://dx.doi.org/10.1016/j.ajpath.2010.11.006

658 41. Osterholzer JJ, Olszewski MA, Murdock BJ, Chen G-H, Erb-Downward JR, Subbotina
659 N, et al. Implicating Exudate Macrophages and Ly-6C high Monocytes in CCR2-
660 Dependent Lung Fibrosis following Gene-Targeted Alveolar Injury . J Immunol.
661 2013;190(7):3447–57.

662 42. Herbold W, Maus R, Hahn I, Ding N, Srivastava M, Christman JW, et al. Importance
663 of CXC chemokine receptor 2 in alveolar neutrophil and exudate macrophage
664 recruitment in response to pneumococcal lung infection. Infect Immun.
665 2010;78(6):2620–30.

666 43. Gelfand EW, Joetham A, Wang M, Takeda K, Schedel M. Spectrum of T-lymphocyte
667 activities regulating allergic lung inflammation. Immunol Rev. 2017 Jul;278(1):63–86.

668 44. Robinson DS. The role of the T cell in asthma. J Allergy Clin Immunol .
669 2010;126(6):1081–91. Available from: http://dx.doi.org/10.1016/j.jaci.2010.06.025

670 45. Akbari O, Stock P, Meyer E, Kronenberg M, Sidobre S, Nakayama T, et al. Essential
671 role of NKT cells producing IL-4 and IL-13 in the development of allergen-induced
672 airway hyperreactivity. Nat Med. 2003;9(5):582–8.

673 46. Akbari O, Umetsu DT. Natural killer T cells and CD8(+) T cells are dispensable for T
674 cell-dependent allergic airway inflammation - Reply. Nat Med. 2006;12(12):1347.

675 47. Lisbonne M, Diem S, de Castro Keller A, Lefort J, Araujo LM, Hachem P, et al. Cutting
676 edge: invariant V alpha 14 NKT cells are required for allergen-induced airway
677 inflammation and hyperreactivity in an experimental asthma model. J Immunol.

2003;171(4):1637–41.

48. Wingender G, Rogers P, Batzer G, Lee MS, Bai D, Pei B, et al. Invariant NKT cells are required for airway inflammation induced by environmental antigens. J Exp Med . 2011;208(6):1151–62. Available from: http://www.jem.org/lookup/doi/10.1084/jem.20102229

49. Lambrecht BN, Hammad H. The immunology of asthma. Nat Immunol . 2014;16(1):45–56. Available from: http://www.ncbi.nlm.nih.gov/pubmed/25521684

50. Wypych TP, Marzi R, Wu GF, Lanzavecchia A, Sallusto F. Role of B cells in TH cell responses in a mouse model of asthma. J Allergy Clin Immunol . 2018;141(4):1395–410. Available from: https://doi.org/10.1016/j.jaci.2017.09.001

51. Foo SY, Phipps S. Regulation of inducible BALT formation and contribution to immunity and pathology. Mucosal Immunol. 2010;3(6):537–44.

52. Marin ND, Dunlap MD, Kaushal D, Khader SA. Friend or Foe: The Protective and Pathological Roles of Inducible Bronchus-Associated Lymphoid Tissue in Pulmonary Diseases. J Immunol. 2019;202(9):2519–26.

53. Radermecker C, Sabatel C, Vanwinge C, Ruscitti C, Maréchal P, Perin F, et al. Locally instructed CXCR4hi neutrophils trigger environment-driven allergic asthma through the release of neutrophil extracellular traps. Nat Immunol . 2019;20(11):1444–55. Available from: http://dx.doi.org/10.1038/s41590-019-0496-9

54. Woo LN, Guo WY, Wang X, Young A, Salehi S, Hin A, et al. A 4-Week Model of House Dust Mite (HDM) Induced Allergic Airways Inflammation with Airway Remodeling. 2018;(December 2017):1–11.

55. Cyphert-Daly JM, Yang Z, Ingram JL, Tighe RM, Que LG. Physiologic response to chronic house dust mite exposure in mice is dependent on lot characteristics. J Allergy Clin Immunol. 2019;144(5):1428-1432.e8.

56. Fallon PG, Schwartz C. The high and lows of type 2 asthma and mouse models. J Allergy Clin Immunol . 2020;145(2):496–8. Available from: https://doi.org/10.1016/j.jaci.2019.11.031

57. Korošec P, Gibbs BF, Rijavec M, Custovic A, Turner PJ. Important and specific role

for basophils in acute allergic reactions. Clin Exp Allergy. 2018;48(5):502–12.

58. Wakahara K, Van VQ, Baba N, Bégin P, Rubio M, Delespesse G, et al. Basophils are recruited to inflamed lungs and exacerbate memory Th2 responses in mice and humans. Allergy Eur J Allergy Clin Immunol. 2013;68(2):180–9.

59. Reber LL, Sibilano R, Mukai K, Galli SJ. Potential effector and immunoregulatory functions of mast cells in mucosal immunity. Mucosal Immunol. 2015;8(3):444–63.

60. Sawaguchi M, Tanaka S, Nakatani Y, Harada Y, Mukai K, Matsunaga Y, et al. Role of Mast Cells and Basophils in IgE Responses and in Allergic Airway Hyperresponsiveness. J Immunol. 2012;188(4):1809–18.

61. Carroll NG, Mutavdzic S, James AL. Distribution and degranulation of airway mast cells in normal and asthmatic subjects. Eur Respir J. 2002;19(5):879–85.

62. Carroll NG. Increased mast cells and neutrophils in submucosal mucous glands and mucus plugging in patients with asthma. Thorax . 2002 Aug 1;57(8):677–82. Available from: https://thorax.bmj.com/lookup/doi/10.1136/thorax.57.8.677

63. Balzar S, Fajt ML, Comhair SAA, Erzurum SC, Bleecker E, Busse WW, et al. Mast cell phenotype, location, and activation in severe asthma: Data from the Severe Asthma Research Program. Am J Respir Crit Care Med. 2011;183(3):299–309.

64. Hammad H, Plantinga M, Deswarte K, Pouliot P, Willart MAM, Kool M, et al. Inflammatory dendritic cells - not basophils - are necessary and sufficient for induction of Th2 immunity to inhaled house dust mite allergen. J Exp Med. 2010;207(10):2097–111.

65. Maazi H, Lam J, Lombardi V, Akbari O. Role of plasmacytoid dendritic cell subsets in allergic asthma. Allergy Eur J Allergy Clin Immunol. 2013;68(6):695–701.

66. Heer HJ De, Hammad H, Soullié T, Hijdra D, Vos N, Willart MAM, et al. Essential Role of Lung Plasmacytoid Dendritic Cells in Preventing Asthmatic Reactions to Harmless Inhaled Antigen. 2004;200(1).

67. Kool M, van Nimwegen M, Willart MAM, Muskens F, Boon L, Smit JJ, et al. An Anti-Inflammatory Role for Plasmacytoid Dendritic Cells in Allergic Airway Inflammation. J Immunol. 2009;183(2):1074–82.

736 68. Lynch JP, Werder RB, Loh Z, Sikder MAA, Curren B, Zhang V, et al. Plasmacytoid
737 dendritic cells protect from viral bronchiolitis and asthma through semaphorin 4a-
738 mediated T reg expansion. J Exp Med. 2018;215(2):537–57.

739 69. Maazi H, Banie H, Aleman Muench GR, Patel N, Wang B, Sankaranarayanan I, et al.
740 Activated plasmacytoid dendritic cells regulate type 2 innate lymphoid cell–mediated
741 airway hyperreactivity. J Allergy Clin Immunol . 2018;141(3):893-905.e6. Available
742 from: http://dx.doi.org/10.1016/j.jaci.2017.04.043

743 70. Bratke K, Lommatzsch M, Julius P, Kuepper M, Kleine HD, Luttmann W, et al.
744 Dendritic cell subsets in human bronchoalveolar lavage fluid after segmental allergen
745 challenge. Thorax. 2007;62(2):168–75.

746 71. Dua B, Watson RM, Gauvreau GM, O'Byrne PM. Myeloid and plasmacytoid dendritic
747 cells in induced sputum after allergen inhalation in subjects with asthma. J Allergy
748 Clin Immunol . 2010;126(1):133–9. Available from:
749 http://dx.doi.org/10.1016/j.jaci.2010.04.006

750 72. Zhou X, Moore BB. Location or origin? What is critical for macrophage propagation
751 of lung fibrosis? Eur Respir J. 2018;51(3):1–4.

752 73. Machado-Aranda D, V. Suresh M, Yu B, Dolgachev V, Hemmila MR, Raghavendran
753 K. Alveolar macrophage depletion increases the severity of acute inflammation
754 following nonlethal unilateral lung contusion in mice. J Trauma Acute Care Surg.
755 2014;76(4):982–90.

756 74. Maus UA, Janzen S, Wall G, Srivastava M, Blackwell TS, Christman JW, et al.
757 Resident alveolar macrophages are replaced by recruited monocytes in response to
758 endotoxin-induced lung inflammation. Am J Respir Cell Mol Biol. 2006;35(2):227–35.

759 75. Mould KJ, Barthel L, Mohning MP, Thomas SM, McCubbrey AL, Danhorn T, et al.
760 Cell origin dictates programming of resident versus recruited macrophages during
761 acute lung injury. Am J Respir Cell Mol Biol. 2017;57(3):294–306.

762 76. Zasłona Z, Przybranowski S, Wilke C, van Rooijen N, Teitz-Tennenbaum S,
763 Osterholzer JJ, et al. Resident Alveolar Macrophages Suppress, whereas Recruited
764 Monocytes Promote, Allergic Lung Inflammation in Murine Models of Asthma. J

765 Immunol. 2014;193(8):4245–53.

766 77. Misharin A V., Morales-Nebreda L, Reyfman PA, Cuda CM, Walter JM, McQuattie-
767 Pimentel AC, et al. Monocyte-derived alveolar macrophages drive lung fibrosis and
768 persist in the lung over the life span. J Exp Med. 2017;214(8):2387–404.

769 78. Sabatel C, Radermecker C, Fievez L, Paulissen G, Chakarov S, Fernandes C, et al.
770 Exposure to Bacterial CpG DNA Protects from Airway Allergic Inflammation by
771 Expanding Regulatory Lung Interstitial Macrophages. Immunity . 2017;46(3):457–73.
772 Available from: http://dx.doi.org/10.1016/j.immuni.2017.02.016

773 79. Meziani L, Mondini M, Petit B, Boissonnas A, De Montpreville VT, Mercier O, et al.
774 CSF1R inhibition prevents radiation pulmonary fibrosis by depletion of interstitial
775 macrophages. Eur Respir J . 2018;51(3):1–13. Available from:
776 http://dx.doi.org/10.1183/13993003.02120-2017

777 80. Lin KL, Suzuki Y, Nakano H, Ramsburg E, Gunn MD. CCR2 + Monocyte-Derived
778 Dendritic Cells and Exudate Macrophages Produce Influenza-Induced Pulmonary
779 Immune Pathology and Mortality . J Immunol. 2008;180(4):2562–72.

780 81. He X, Qian Y, Li Z, Fan EK, Li Y, Wu L, et al. TLR4-Upregulated IL-1β and IL-1RI
781 Promote Alveolar Macrophage Pyroptosis and Lung Inflammation through an
782 Autocrine Mechanism. Sci Rep . 2016;6(April):1–11. Available from:
783 http://dx.doi.org/10.1038/srep31663

784 82. Al-Ramli W, Préfontaine D, Chouiali F, Martin JG, Olivenstein R, Lemière C, et al.
785 TH17-associated cytokines (IL-17A and IL-17F) in severe asthma. J Allergy Clin
786 Immunol. 2009;123(5):1185–7.

787 83. Ghosh S, Hoselton SA, Asbach S V., Steffan BN, Wanjara SB, Dorsam GP, et al. B
788 lymphocytes regulate airway granulocytic inflammation and cytokine production in a
789 murine model of fungal allergic asthma. Cell Mol Immunol. 2015;12(2):202–12.

790 84. Shinoda K, Hirahara K, Nakayama T. Maintenance of pathogenic Th2 cells in allergic
791 disorders. Allergol Int . 2017;66(3):369–76. Available from:
792 http://dx.doi.org/10.1016/j.alit.2017.03.005

793 85. Hirahara K, Shinoda K, Endo Y, Ichikawa T, Nakayama T. Maintenance of memory-

type pathogenic Th2 cells in the pathophysiology of chronic airway inflammation. Inflamm Regen. 2018;38(1):8–11.

86. Wingender G, Birkholz a. M, Sag D, Farber E, Chitale S, Howell a. R, et al. Selective Conditions Are Required for the Induction of Invariant NKT Cell Hyporesponsiveness by Antigenic Stimulation. J Immunol . 2015;195(8):3838–48. Available from: http://www.jimmunol.org/cgi/doi/10.4049/jimmunol.1500203

87. Roederer M, Darzynkiewicz Z, Parks DR. Guidelines for the presentation of flow cytometric data. Methods Cell Biol. 2004;2004(75):241–56.

88. Moro K, Ealey KN, Kabata H, Koyasu S. Isolation and analysis of group 2 innate lymphoid cells in mice. Nat Protoc . 2015;10(5):792–806. Available from: http://dx.doi.org/10.1038/nprot.2015.047

89. Kuroda E, Ozasa K, Temizoz B, Ohata K, Koo CX, Kanuma T, et al. Inhaled Fine Particles Induce Alveolar Macrophage Death and Interleukin-1α Release to Promote Inducible Bronchus-Associated Lymphoid Tissue Formation. Immunity . 2016;45(6):1299–310. Available from: http://linkinghub.elsevier.com/retrieve/pii/S1074761316304824

90. Maecker HT. Multiparameter Flow Cytometry Monitoring of T Cell Responses. In: Prasad VR, Kalpana G V, editors. HIV Protocols . Totowa, NJ: Humana Press; 2009. p. 375–91. Available from: https://doi.org/10.1007/978-1-59745-170-3_25

Supplemental figure legends

S1 Fig: Gating strategy to identify myeloid cells in the inflamed lung. A graphic outline **(A)** and exemplary graphs **(B)** are given to illustrate the gating strategy employed to identify myeloid cells in the lung and BALF. Alveolar macrophages (AMs): live CD45$^+$ CD19$^-$ Siglec-F$^+$ Ly6G$^-$ CD11c$^+$ cells; Basophils: live CD45$^+$ CD19$^-$ Siglec-F$^-$ Ly6G$^-$ CD11b$^+$ FcεRIα$^+$ CD117$^-$ cells; Conventional DCs (cDC): live CD45$^+$ CD19$^-$ Siglec-F$^-$ Ly6G$^-$ CD24$^+$ CD11c$^+$ MHC class II$^+$ CD103$^-$ CD11b$^+$ cells; CD103$^+$ DCs: live CD45$^+$ CD19$^-$ Siglec-F$^-$ Ly6G$^-$ CD24$^+$ CD11c$^+$ MHC class II$^+$ CD103$^+$ cells; Dendritic cells (all): live CD19$^-$ CD45$^+$ Siglec-F$^-$ Ly6G$^-$ F4/80$^-$ CD64$^-$ CD24$^+$ CD11c$^+$ MHC class II$^{+/-}$; Eosinophils: live CD45$^+$ CD19$^-$ CD11c$^-$ CD11b$^-$ Ly6G$^-$ Siglec-F$^+$ cells; Exudate macrophages (ExMs): live CD45$^+$ CD19$^-$ Siglec-F$^-$ Ly6G$^-$ CD24$^-$ F4/80$^+$ CD64$^{+/-}$ Ly6C$^+$ CD11b$^+$ cells; Interstitial macrophages (IMs): live CD45$^+$ CD19$^-$ Siglec-F$^-$ Ly6G$^-$ CD24$^-$ F4/80$^+$ CD64$^{+/-}$ Ly6C$^+$ CD11b$^-$ cells; Neutrophils: live CD45$^+$ CD19$^-$ CD11b$^{+/lo}$ Ly6G$^+$ cells; Macrophages (all): live CD19$^-$ CD45$^+$ Siglec-F$^-$ Ly6G$^-$ F4/80$^+$ CD64$^+$ cells; Mast cells: live CD45$^+$ CD19$^-$ Siglec-F$^-$ Ly6G$^-$ CD11b$^+$ FcεRIα$^+$ CD117$^+$ cells; Plasmacytoid dendritic cells: pDC, live CD19$^-$ CD45$^+$ Siglec-F$^-$ Ly6G$^-$ CD11b$^-$ CD45R$^+$ Ly6C$^+$ cells.

S2 Fig: Gating strategy to identify lymphoid cells in the inflamed lung. A graphic outline **(A)** and exemplary graphs **(B)** are given to illustrate the gating strategy employed to identify lymphoid cells in the lung and BALF. Th1 cells (live CD19/CD45R$^-$ CD3ε$^+$ CD4$^+$ Tbet$^+$ cells), Th2 cells (live CD19/B220$^-$ CD3ε$^+$ CD4$^+$ Gata3$^+$ cells), Th17 cells (live CD19/CD45R$^-$ CD3ε$^+$ CD4$^+$ RORγt$^+$ cells), and Tregs (live CD19/CD45R$^-$ CD3ε$^+$ CD4$^+$ CD127$^{lo/-}$ FoxP3$^+$), *i*NKT cells (live CD19/CD45R$^-$ CD3ε$^+$ CD1d/PBS57-tetramer$^+$ cells) and its subsets in the lung NKT1 (PLZF^{lo} RORγt$^-$), NKT2 cells (PLZF$^{int/hi}$ RORγt$^-$), NKT17 cells (PLZF^{int} RORγt$^+$) cells are shown.

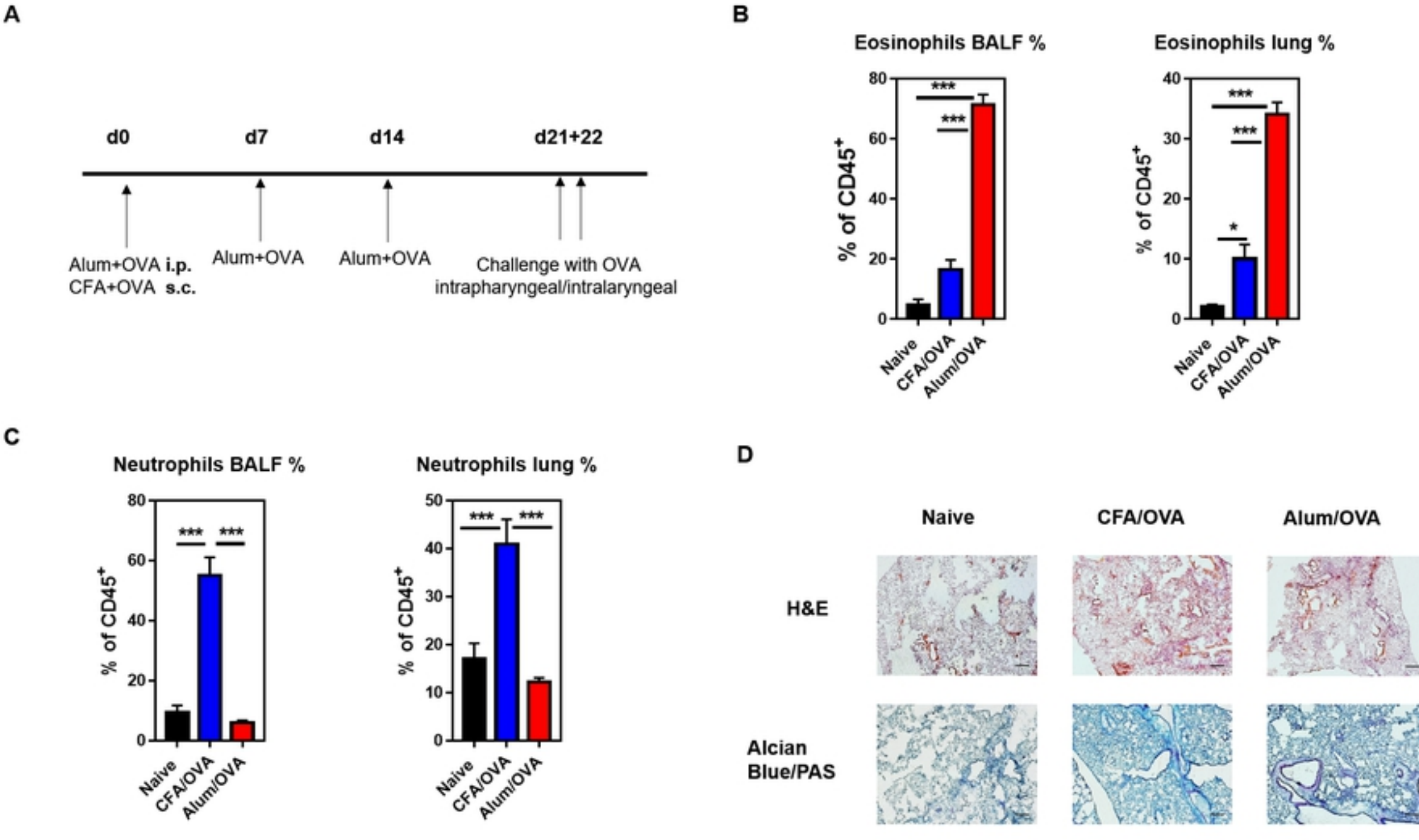
A
d0
d7
d14
d21+22
Alum+OVA i.p.
CFA+OVA s.c.
Alum+OVA
Alum+OVA
Challenge with OVA
intrapharyngeal/intralaryngeal
B
Eosinophils BALF %
% of CD45+
Naive
CFA/OVA
Alum/OVA
Eosinophils lung %
% of CD45+
Naive
CFA/OVA
Alum/OVA
C
Neutrophils BALF %
% of CD45+
Naive
CFA/OVA
Alum/OVA
Neutrophils lung %
% of CD45+
Naive
CFA/OVA
Alum/OVA
D
Naive
CFA/OVA
Alum/OVA
H&E
Alcian
Blue/PAS

Fig 1 A-D

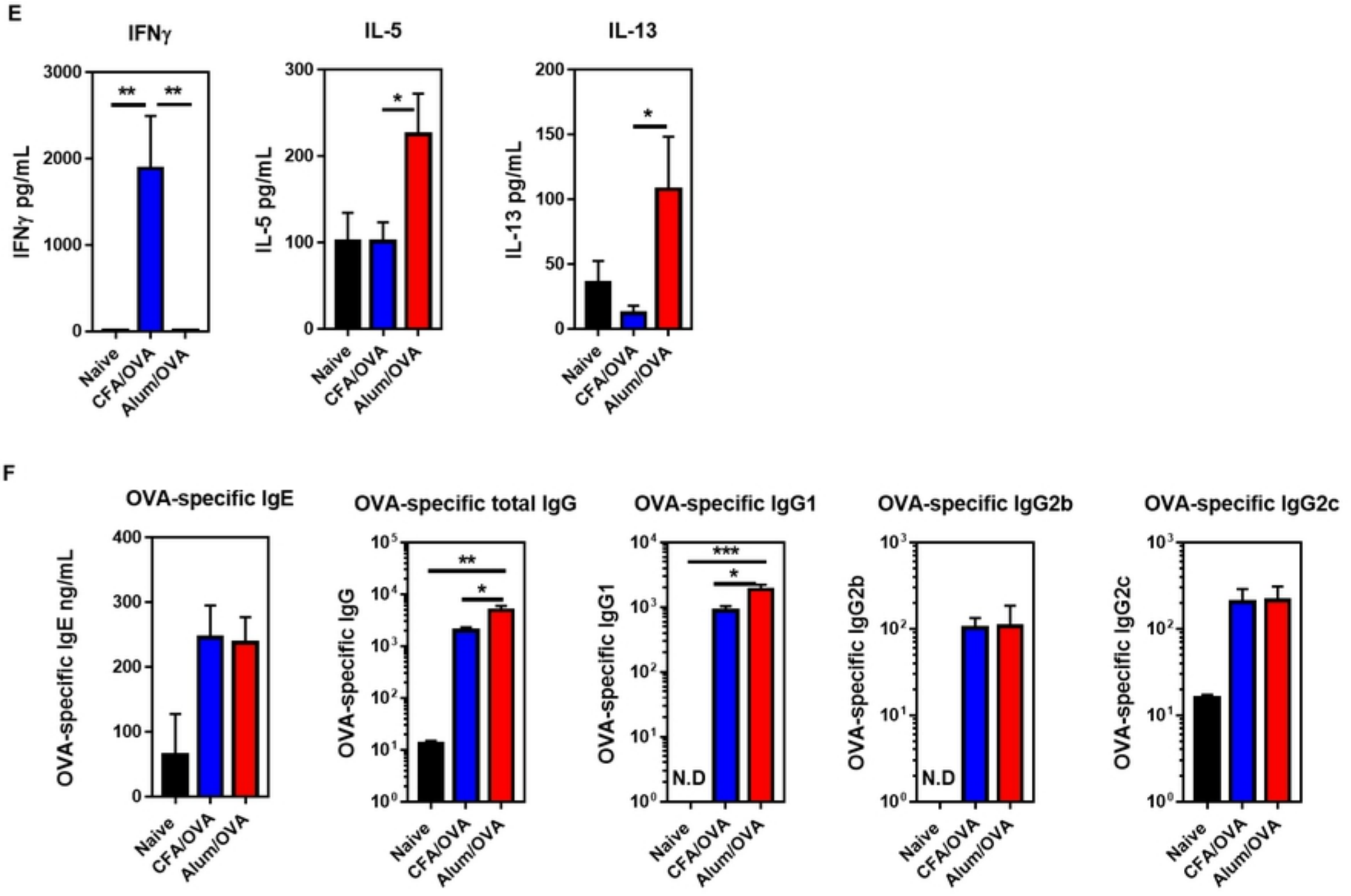
E
IFNγ
IL-5
IL-13
IFNγ pg/mL
IL-5 pg/mL
IL-13 pg/mL
3000
2000
1000
0
300
200
100
0
200
150
100
50
0
**
**
*
*
Naive
CFA/OVA
Alum/OVA
F
OVA-specific IgE
OVA-specific total IgG
OVA-specific IgG1
OVA-specific IgG2b
OVA-specific IgG2c
OVA-specific IgE ng/mL
OVA-specific IgG
OVA-specific IgG1
OVA-specific IgG2b
OVA-specific IgG2c
400
300
200
100
0
10^5
10^4
10^3
10^2
10^1
10^0
10^4
10^3
10^2
10^1
10^0
10^3
10^2
10^1
10^0
10^3
10^2
10^1
10^0
**
*
***
*
N.D
N.D
Naive
CFA/OVA
Alum/OVA

Fig 1 E-F

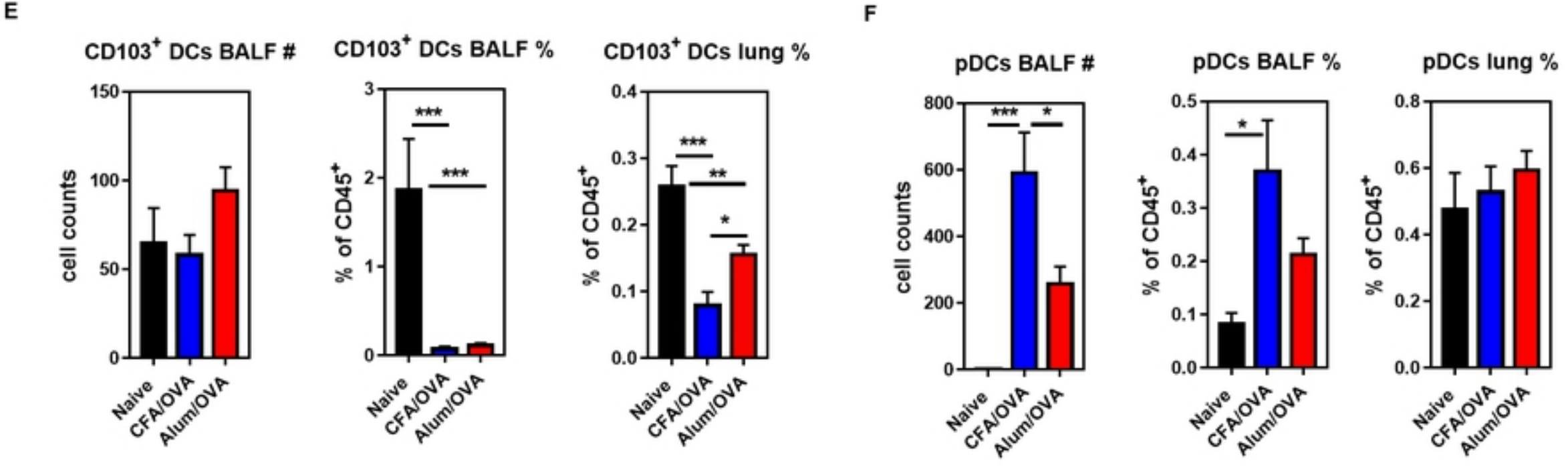
E
CD103+ DCs BALF #
cell counts
150
100
50
0
Naive
CFA/OVA
Alum/OVA
CD103+ DCs BALF %
% of CD45+
3
2
1
0
***
***
Naive
CFA/OVA
Alum/OVA
CD103+ DCs lung %
% of CD45+
0.4
0.3
0.2
0.1
0.0
***
**
*
Naive
CFA/OVA
Alum/OVA
F
pDCs BALF #
cell counts
800
600
400
200
0
***
*
Naive
CFA/OVA
Alum/OVA
pDCs BALF %
% of CD45+
0.5
0.4
0.3
0.2
0.1
0.0
*
Naive
CFA/OVA
Alum/OVA
pDCs lung %
% of CD45+
0.8
0.6
0.4
0.2
0.0
Naive
CFA/OVA
Alum/OVA

Fig 2 E-F

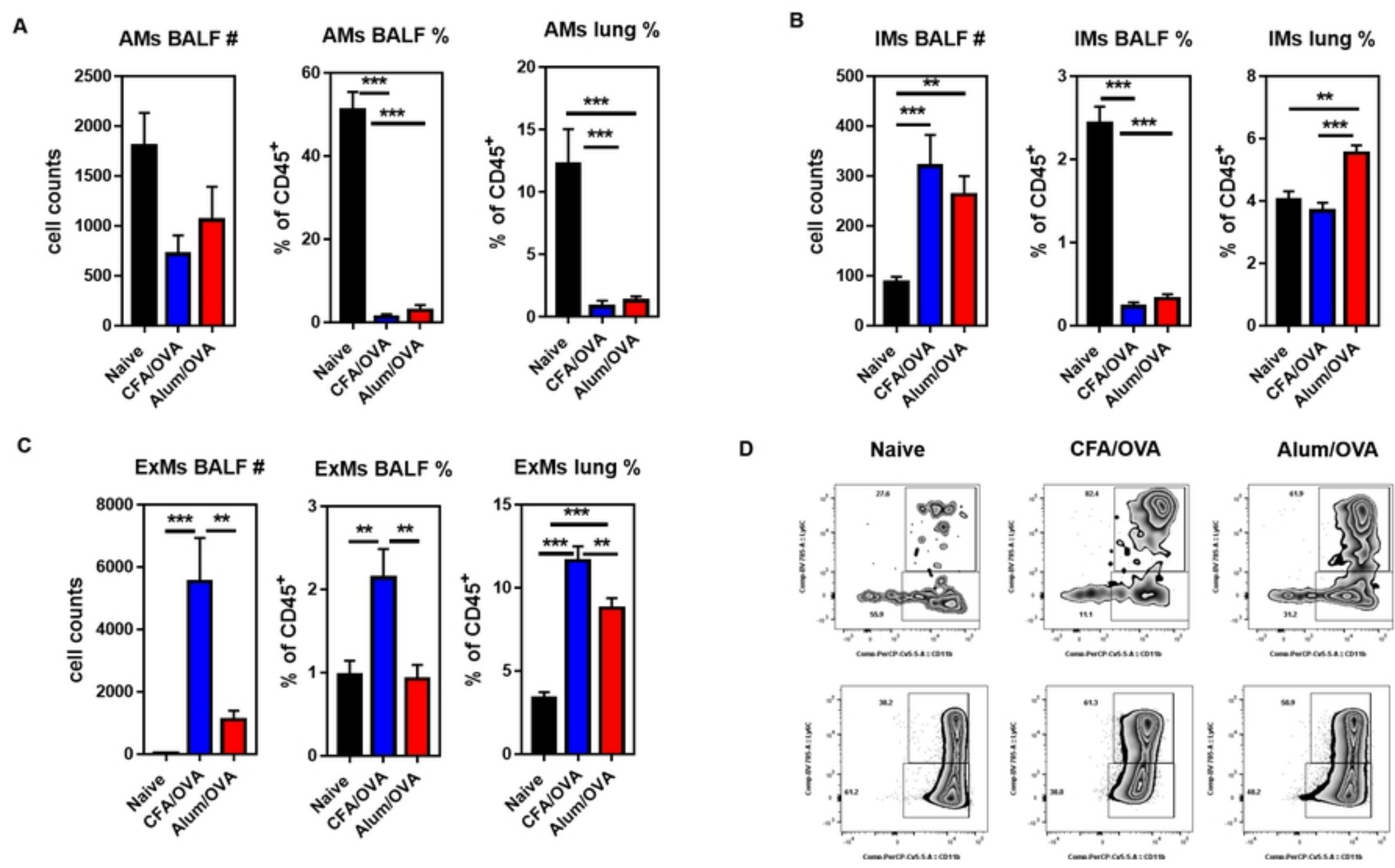
A
AMs BALF #
AMs BALF %
AMs lung %
cell counts
% of CD45+
Naive
CFA/OVA
Alum/OVA
B
IMs BALF #
IMs BALF %
IMs lung %
C
ExMs BALF #
ExMs BALF %
ExMs lung %
D
Naive
CFA/OVA
Alum/OVA

Fig 3 A-D

E

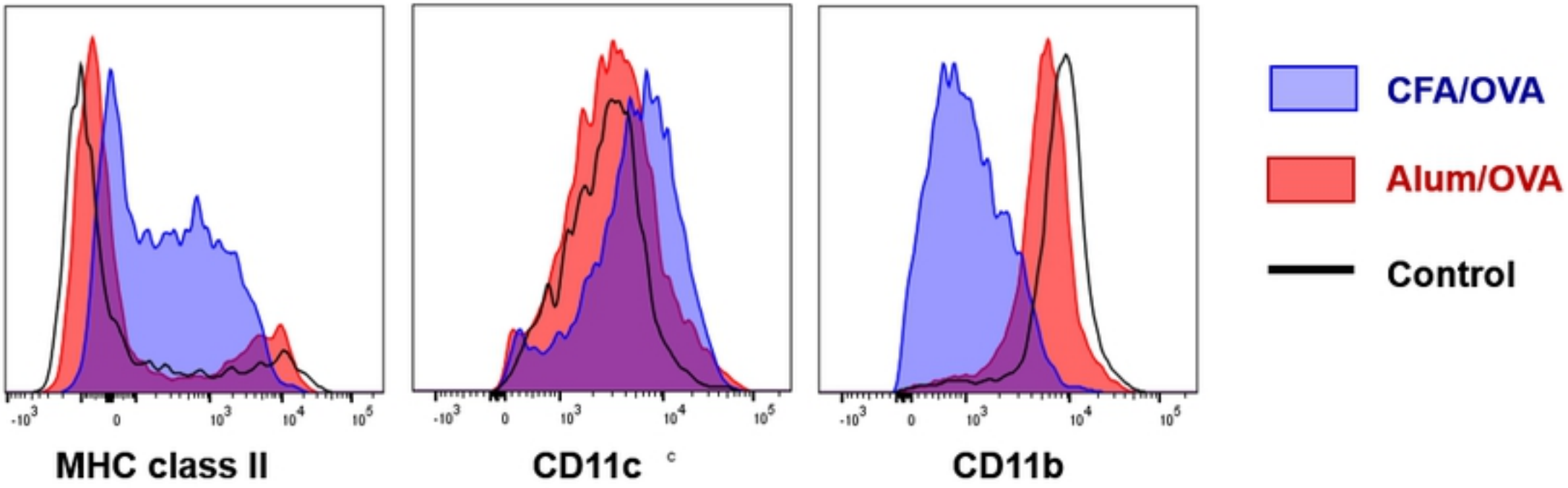

F

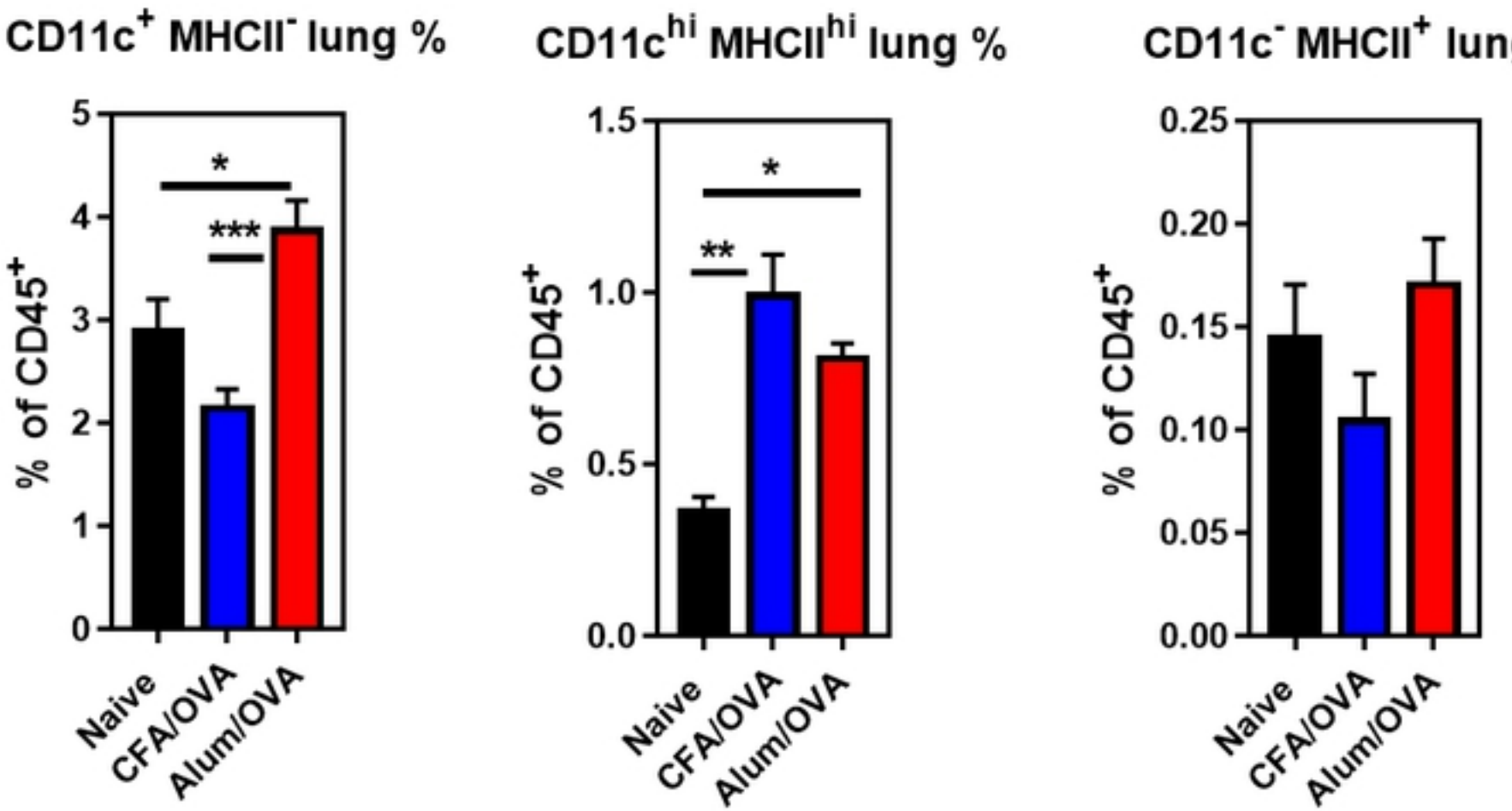

Fig 3 E-F

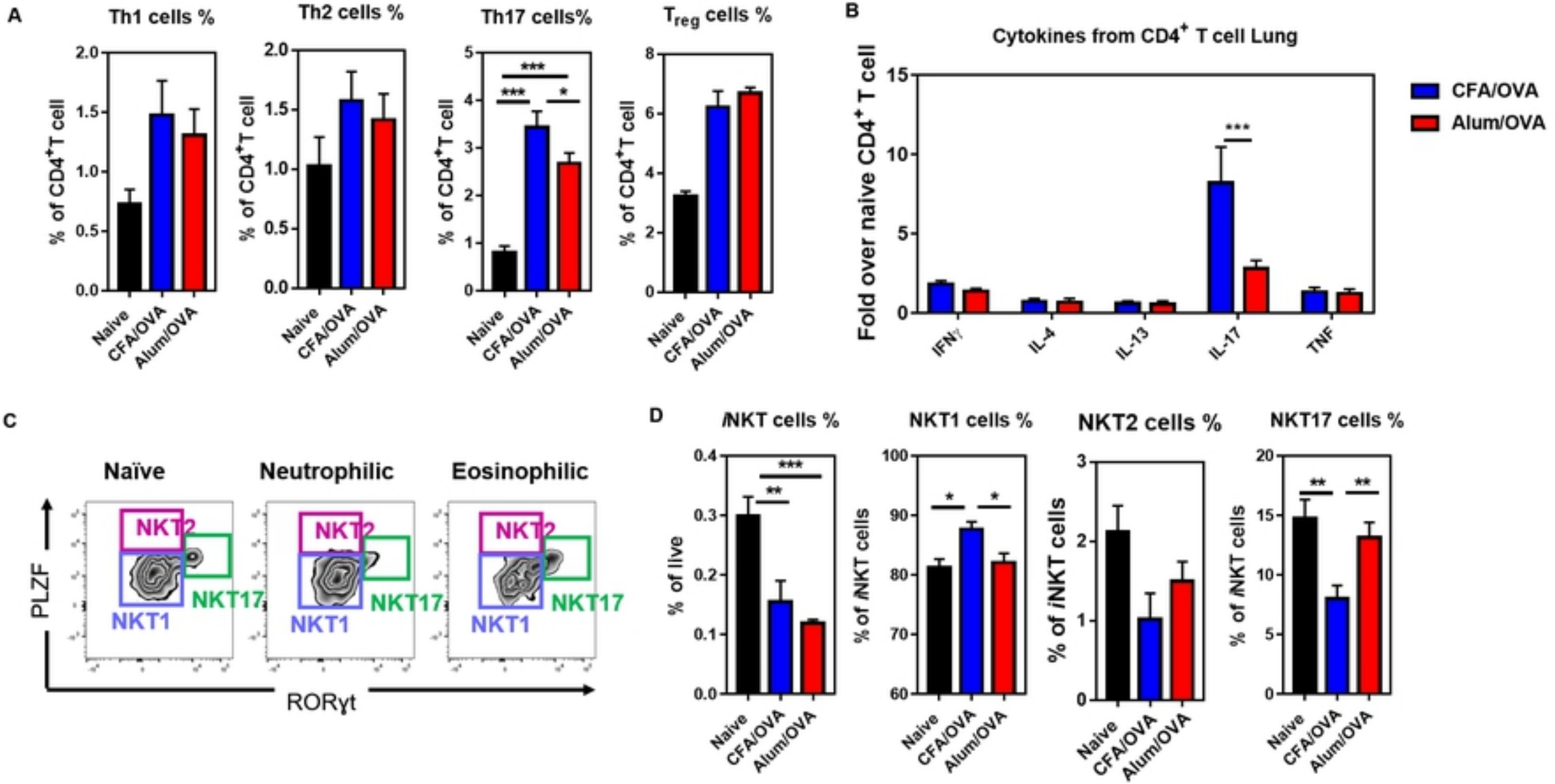
A
Th1 cells %
Th2 cells %
Th17 cells%
T_{reg} cells %
% of CD4+T cell
Naive
CFA/OVA
Alum/OVA
B
Cytokines from CD4+ T cell Lung
Fold over naive CD4+ T cell
IFNγ
IL-4
IL-13
IL-17
TNF
CFA/OVA
Alum/OVA
C
Naïve
Neutrophilic
Eosinophilic
NKT2
NKT17
NKT1
PLZF
RORγt
D
iNKT cells %
NKT1 cells %
NKT2 cells %
NKT17 cells %
% of live
% of iNKT cells

Fig 4

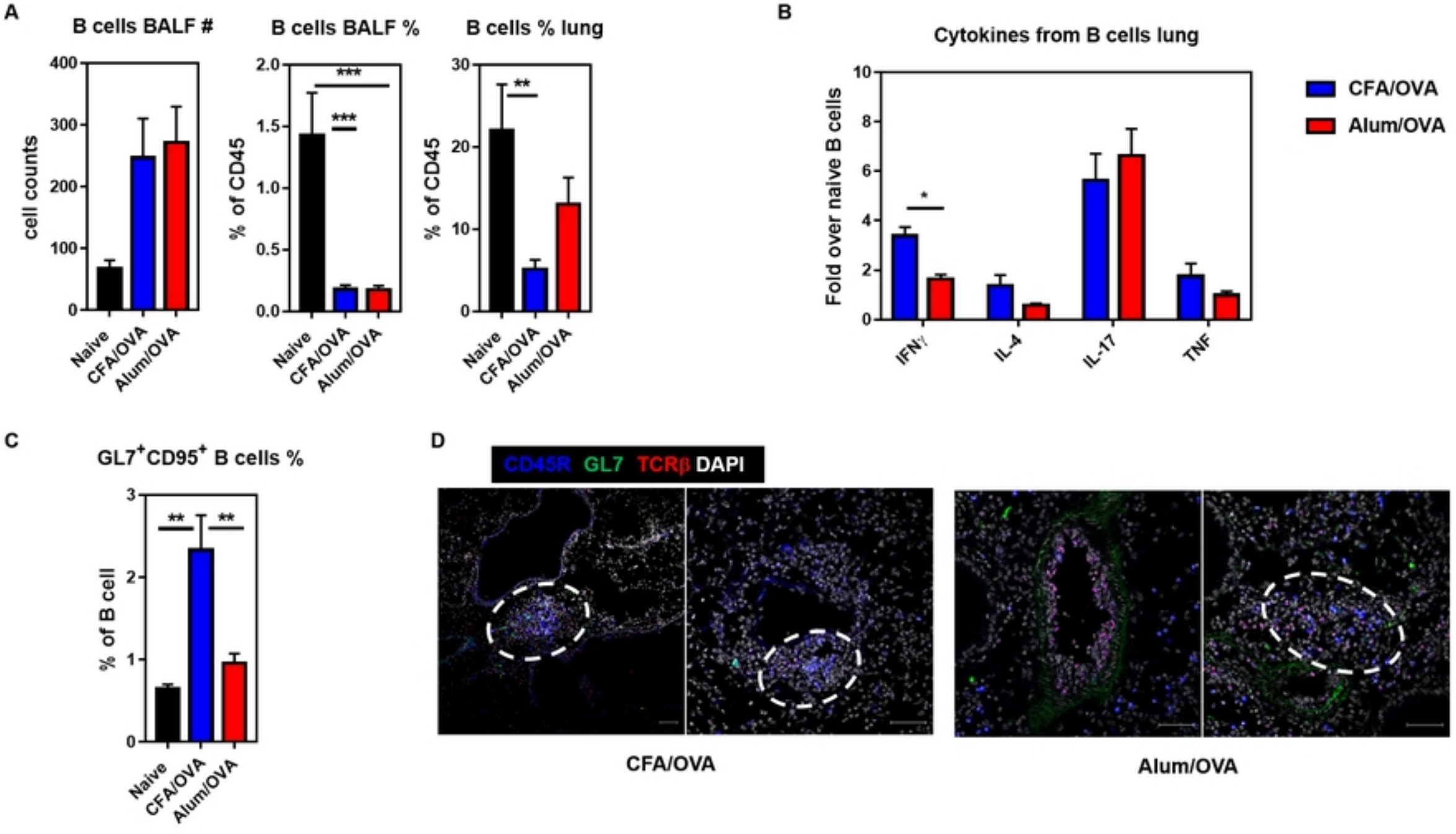
A
B cells BALF #
cell counts
400
300
200
100
0
Naive
CFA/OVA
Alum/OVA
B cells BALF %
% of CD45
2.0
1.5
1.0
0.5
0.0
***
***
B cells % lung
30
20
10
0
**
B
Cytokines from B cells lung
Fold over naive B cells
10
8
6
4
2
0
*
IFNγ
IL-4
IL-17
TNF
CFA/OVA
Alum/OVA
C
GL7+CD95+ B cells %
% of B cell
3
2
1
0
**
**
D
CD45R GL7 TCRβ DAPI
CFA/OVA
Alum/OVA

Fig 5

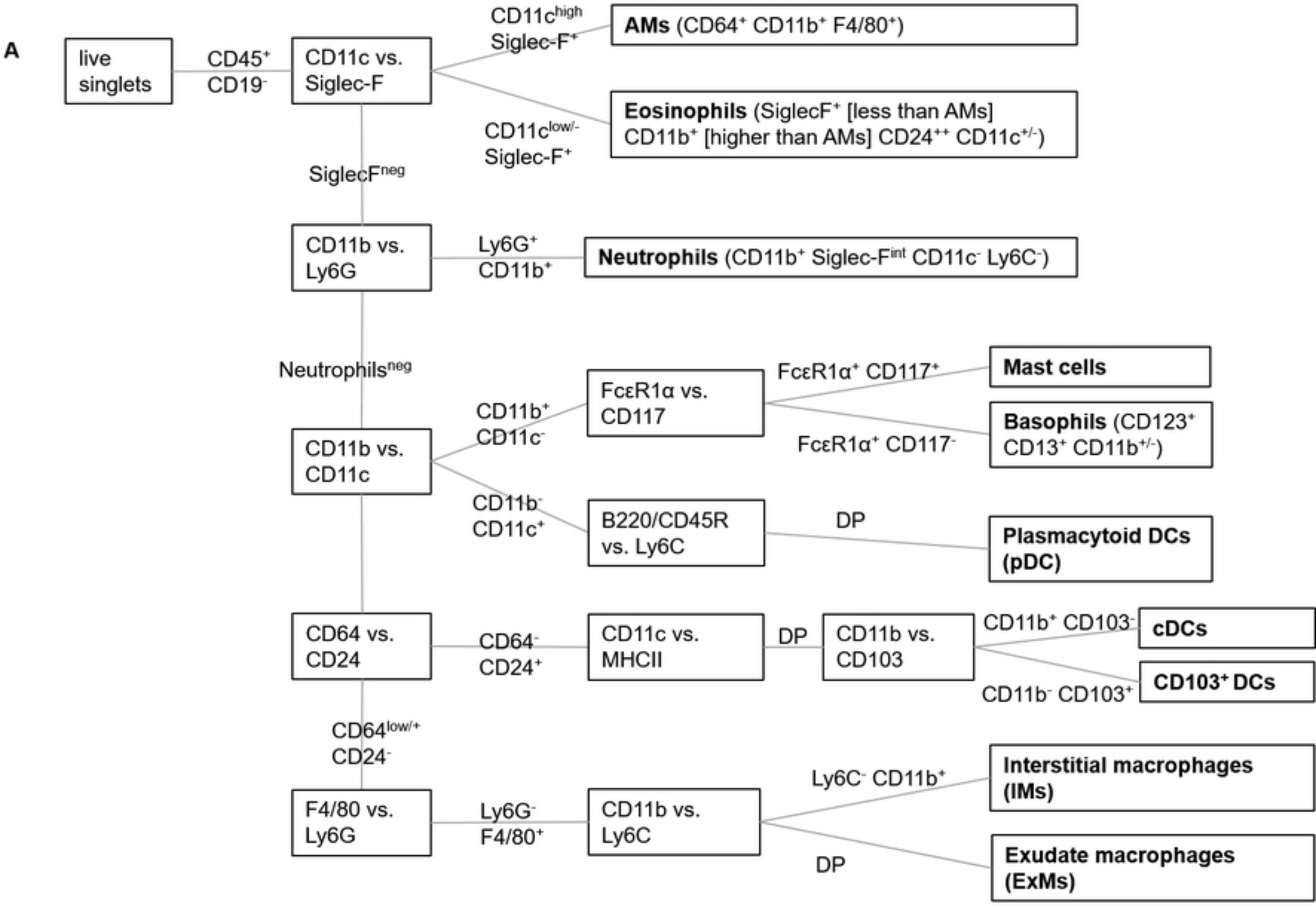
A
live singlets
CD45+ CD19-
CD11c vs. Siglec-F
CD11chigh Siglec-F+
AMs (CD64+ CD11b+ F4/80+)
CD11clow/- Siglec-F+
Eosinophils (SiglecF+ [less than AMs] CD11b+ [higher than AMs] CD24++ CD11c+/-)
SiglecFneg
CD11b vs. Ly6G
Ly6G+ CD11b+
Neutrophils (CD11b+ Siglec-Fint CD11c- Ly6C-)
Neutrophilsneg
CD11b vs. CD11c
CD11b+ CD11c-
FcεR1α vs. CD117
FcεR1α+ CD117+
Mast cells
FcεR1α+ CD117-
Basophils (CD123+ CD13+ CD11b+/-)
CD11b- CD11c+
B220/CD45R vs. Ly6C
DP
Plasmacytoid DCs (pDC)
CD64 vs. CD24
CD64- CD24+
CD11c vs. MHCII
DP
CD11b vs. CD103
CD11b+ CD103-
cDCs
CD11b- CD103+
CD103+ DCs
CD64low/+ CD24-
F4/80 vs. Ly6G
Ly6G- F4/80+
CD11b vs. Ly6C
Ly6C- CD11b+
Interstitial macrophages (IMs)
DP
Exudate macrophages (ExMs)

S1 Fig A

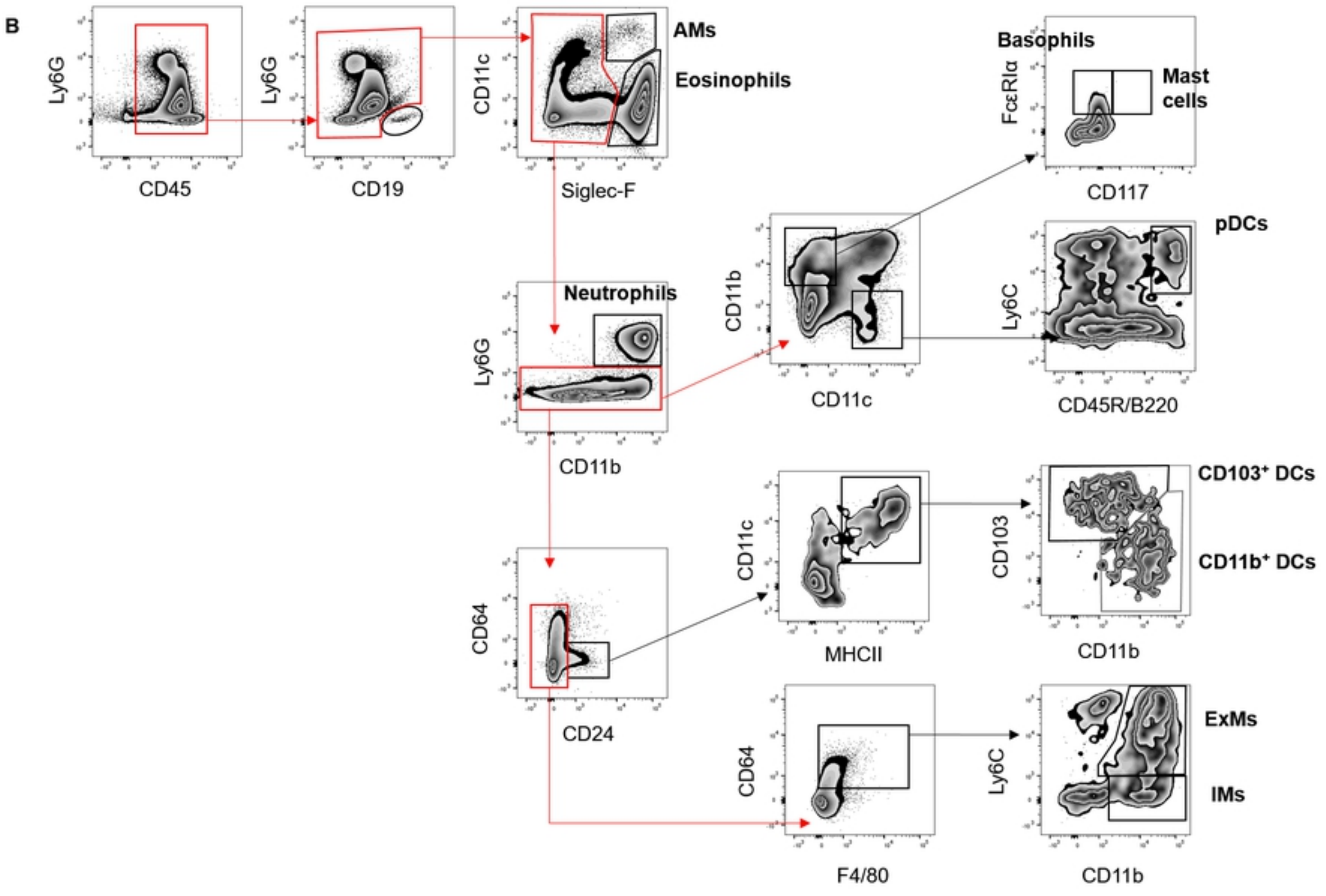
B
Ly6G
CD45
Ly6G
CD19
CD11c
Siglec-F
AMs
Eosinophils
Basophils
FcεRIα
Mast cells
CD117
pDCs
Ly6C
CD45R/B220
CD11b
CD11c
Neutrophils
Ly6G
CD11b
CD64
CD24
CD11c
MHCII
CD103
CD103⁺ DCs
CD11b⁺ DCs
CD11b
CD64
F4/80
Ly6C
ExMs
IMs
CD11b

S1 Fig B

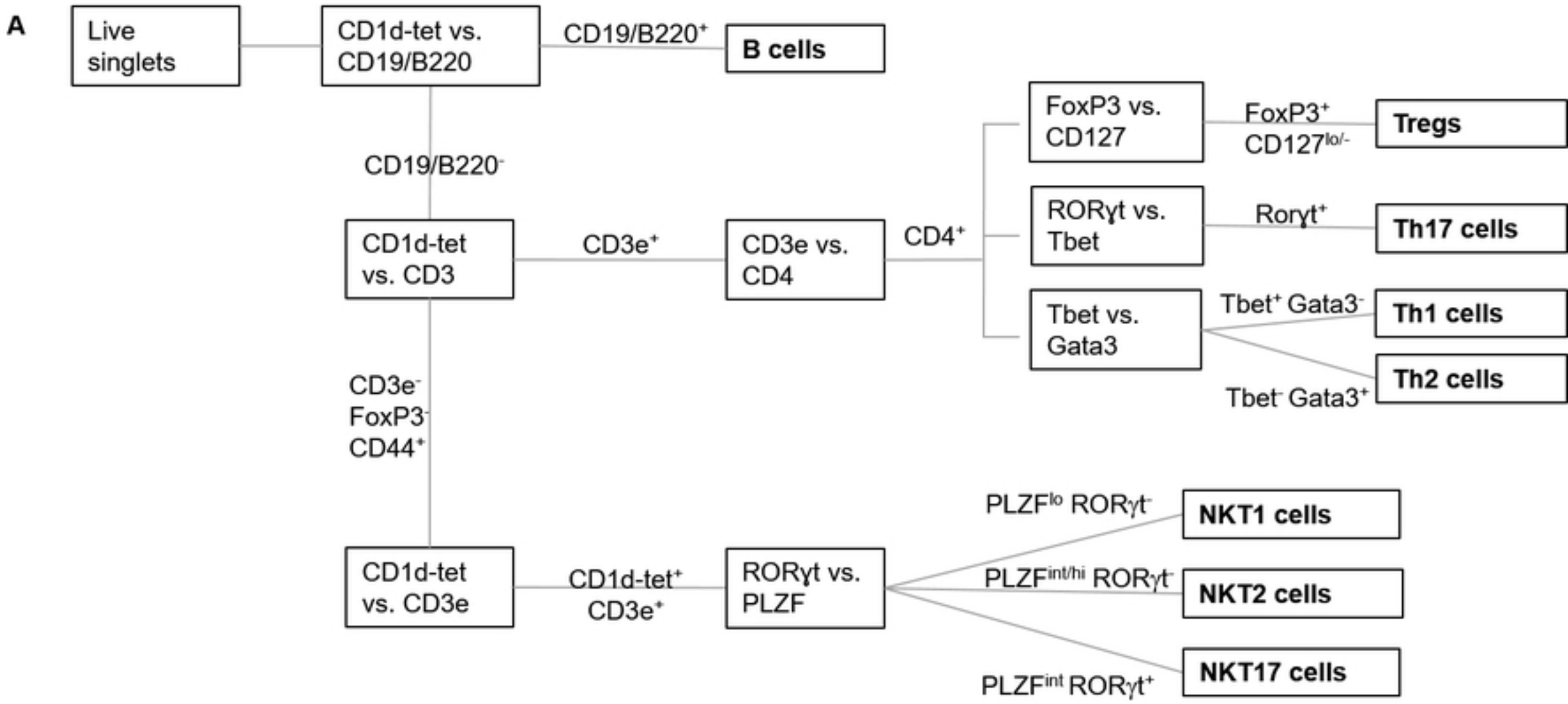
A
Live singlets
CD1d-tet vs. CD19/B220
CD19/B220+
B cells
CD19/B220-
CD1d-tet vs. CD3
CD3e+
CD3e vs. CD4
CD4+
FoxP3 vs. CD127
FoxP3+ CD127lo/-
Tregs
RORγt vs. Tbet
Rorγt+
Th17 cells
Tbet vs. Gata3
Tbet+ Gata3-
Th1 cells
Tbet- Gata3+
Th2 cells
CD3e- FoxP3- CD44+
CD1d-tet vs. CD3e
CD1d-tet+ CD3e+
RORγt vs. PLZF
PLZFlo RORγt-
NKT1 cells
PLZFint/hi RORγt-
NKT2 cells
PLZFint RORγt+
NKT17 cells

S2 Fig A

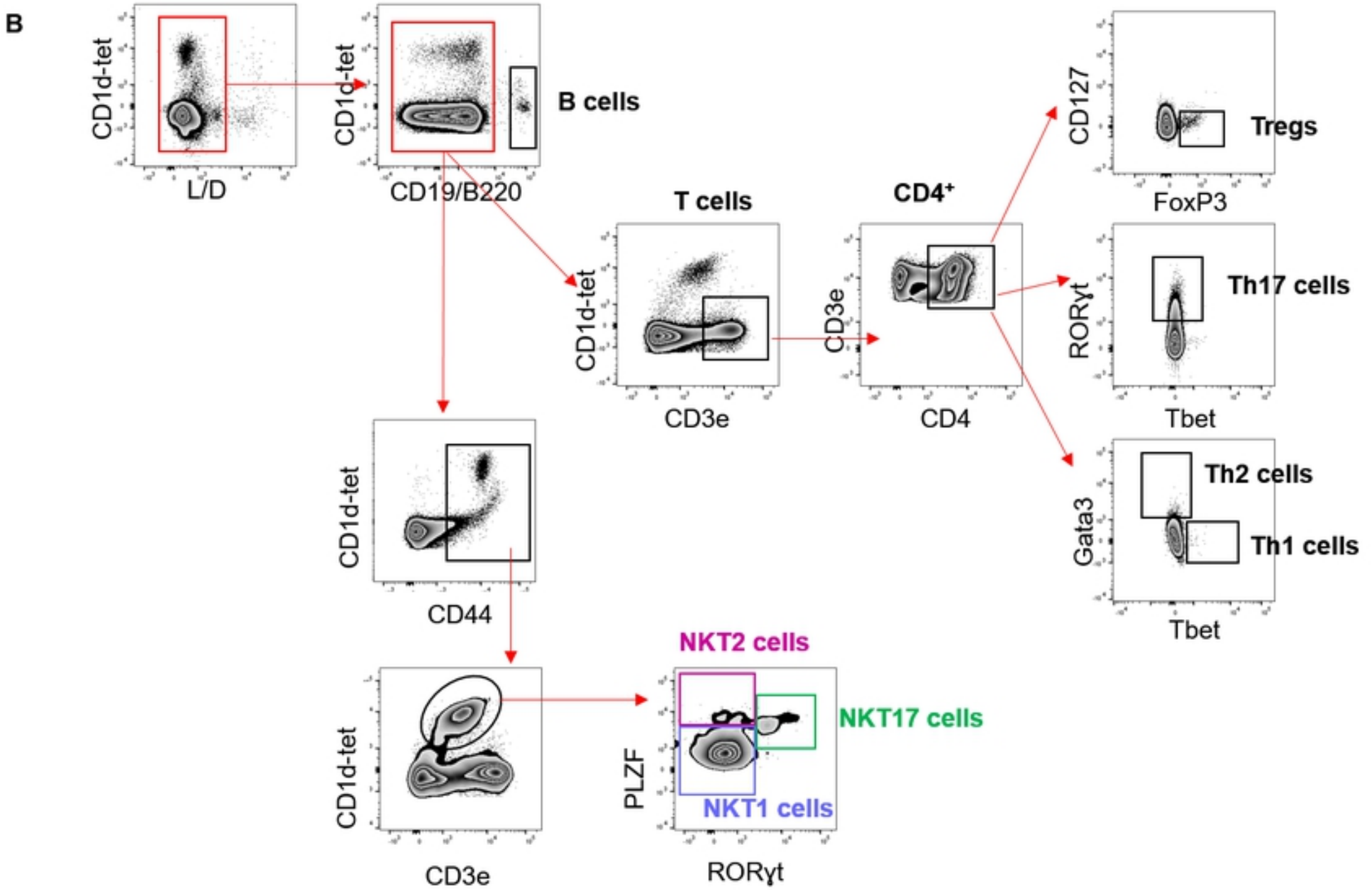
B
CD1d-tet
L/D
CD1d-tet
CD19/B220
B cells
T cells
CD1d-tet
CD3e
CD4+
CD3e
CD4
CD127
FoxP3
Tregs
RORγt
Tbet
Th17 cells
Gata3
Tbet
Th2 cells
Th1 cells
CD1d-tet
CD44
CD1d-tet
CD3e
NKT2 cells
NKT17 cells
NKT1 cells
PLZF
RORγt

S2 Fig B

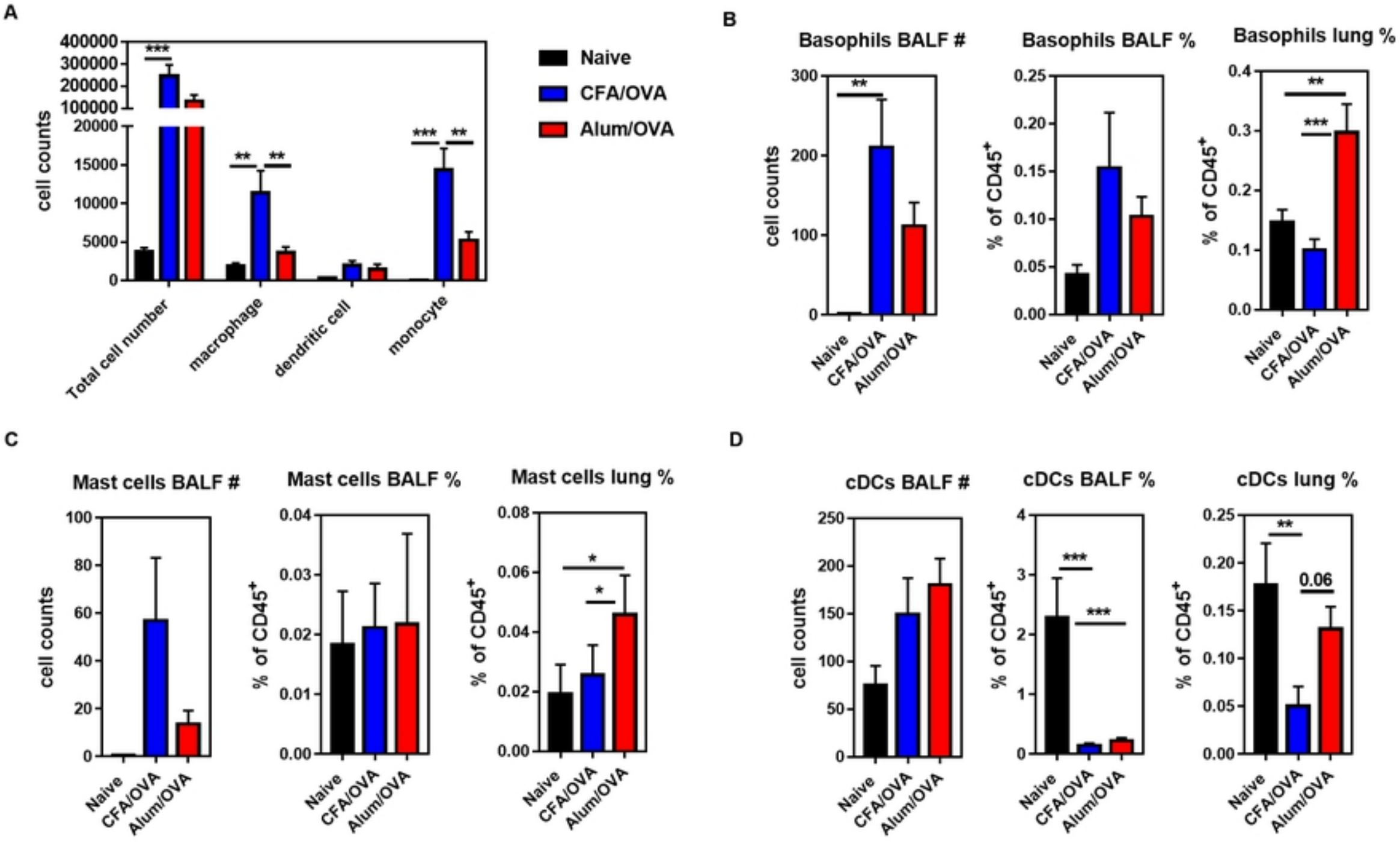
A
cell counts
Total cell number
macrophage
dendritic cell
monocyte
Naive
CFA/OVA
Alum/OVA
B
Basophils BALF #
Basophils BALF %
Basophils lung %
% of CD45+
C
Mast cells BALF #
Mast cells BALF %
Mast cells lung %
D
cDCs BALF #
cDCs BALF %
cDCs lung %
0.06

Fig 2 A-D